THE ASTROPHYSICAL JOURNAL, 468:241–260, 1996 September 1

STELLAR VARIABILITY IN THE CENTRAL POPULATIONS OF 47 TUCANAE FROM WF/PC OBSERVATIONS WITH THE *HUBBLE SPACE TELESCOPE*. II. BINARY SYSTEMS[1]

PETER D. EDMONDS AND RONALD L. GILLILAND
Space Telescope Science Institute,[2] 3700 San Martin Drive, Baltimore, MD 21218; pedmonds@stsci.edu, gillil@stsci.edu
PURAGRA GUHATHAKURTA
University of California, Lick Observatory, Santa Cruz, CA 95064
AND
LARRY D. PETRO, ABHIJIT SAHA, AND MICHAEL M. SHARA
Space Telescope Science Institute,[2] 3700 San Martin Drive, Baltimore, MD 21218
Received 1995 October 31; accepted 1996 March 14

ABSTRACT

Stars in the core of 47 Tuc have been intensively surveyed for variability, using differential time series photometry, with the Planetary Camera of the *Hubble Space Telescope*. Some 20,000 stars were surveyed in the U band (F336W) in a $66'' \times 66''$ field centered on the core of 47 Tuc, with almost continuous observing over 38.5 hr, and using 1000 s exposure times. Using aperture photometry, PSF fitting, and power spectrum techniques, two W UMa systems were discovered, as well as six semidetached or detached binaries with periods between 0.41 and 1.5 days. The two faintest variables found are within the error circles of two highly variable X-ray sources and are good candidates for neutron star binaries or magnetic cataclysic variables. Two other certain variables were found, one of which is a possible cataclysmic variable. The radial distribution of the binaries is significantly more centrally concentrated than the average star, but it is consistent with the radial distribution of the blue stragglers found in the core. We show that the contact binary frequency and the period distribution of the binaries imply that few, if any, of the binaries are primordial.

Subject headings: binaries: close — binaries: eclipsing — globular clusters: individual (47 Tucanae) — novae, cataclysmic variables — stars: statistics — surveys

1. INTRODUCTION

The study of globular clusters (GCs) encompasses many diverse areas of research. For the study of stellar dynamics, GCs provide a unique laboratory for studying systems with enormous stellar densities. GCs simplify calculations in stellar evolution by offering large samples of stars with homogenous ages and chemical compositions, and in statistical mechanics they expose the theoretical limitations in the statistical descriptions of dynamical systems (Meylan, Dubath, & Mayor 1991). Finally, developments in hardware and software are becoming vital in performing full star-by-star simulations of GCs (Hut 1993).

Binaries play a crucial role in the evolution of GCs. Simple calculations suggest that the internal energy reservoir in binary binding energies may exceed the total amount of kinetic energy in a GC (Hut 1993). During stellar encounters, binaries can become more tightly bound and the energy difference can be given up to passing stars. This "burning" of primordial binaries can support a cluster against core collapse for billions of years, and it may also act as a central energy source halting the evolution toward higher central densities during and after core collapse (Hut et al. 1992).

There are two key predictions made by simulations of cluster dynamical evolution (Hut et al. 1992). First, binaries should be more concentrated toward centers of GCs than single stars, since they are heavier than the average star and should sink toward the cluster core on a local relaxation timescale. Much of the initial collapse of a cluster is believed to be driven by binary segregation (Hut et al. 1992). Second, many primordial binaries should be destroyed over a Hubble time in a typical dense cluster.

Observational tests of these two predictions are almost nonexistent, largely because the crowding present in ground-based images of GCs makes it difficult to find binaries. These problems are particularly severe at the centers of the denser GCs, where the densities can exceed $10^5\ M_\odot\ \mathrm{pc}^{-3}$ and the stellar separations, in projection, are typically only a few tenths of an arcsecond. Dense GCs are, however, particularly interesting because they are likely environments for stellar collisions (including multiple exchanges), tidal mergers, and binary disruptions and coalescence.

Since 47 Tuc is closer to the Sun than most Galactic GCs, and since it has a high Galactic latitude, it represents an excellent target for the study of close binaries and blue straggler stars (BSS). In addition, 47 Tuc is a dense cluster and is a known prolific breeding environment for objects likely to be formed by stellar collisions and binary mergers or coalescence. Its core contains a diversity of exotic objects, including: a total of 11 ms pulsars (Manchester et al. 1991), at least three of which are in binaries; five X-ray sources (Verbunt et al. 1993; Hasinger, Johnston, & Verbunt 1994); and two stars with velocities of the order or larger than the central escape velocity of 47 Tuc (Meylan et al. 1991). BSS have also been found in the core of 47 Tuc using the *Hubble Space Telescope* (*HST*): Paresce et al. (1991) discovered 21 BSS, and Guhathakurta et al. (1992),

[1] Based on observations with the NASA/ESA *Hubble Space Telescope*, obtained at the Space Telescope Science Institute, which is operated by Association of Universities for Research in Astronomy, Inc., under NASA contract NAS 5-26555.

[2] Operated by the Association of Universities for Research in Astronomy, Inc., under contract with the National Aeronautics and Space Administration.

using different filters, discovered 24 BSS and showed that their distribution was more centrally concentrated than the giant stars. Finally, evidence has been found for cataclysmic variables (CVs) in the core of 47 Tuc. Paresce & De Marchi (1994) have detected a dwarf nova, and Paresce, De Marchi, & Ferraro (1992) and Shara et al. (1996) have discovered CV candidates. Only two other confirmed CVs are known in other GCs: V101 in M80 (Machin et al. 1990) and the nova of 1860 A.D., also in M80 (Shara & Drissen 1995).

All of the astrophysical objects listed above are thought to be related to binary stars, yet, with the exception of the dwarf nova and binary pulsars, no direct evidence for binaries has been found in the core of 47 Tuc. Furthermore, searches for binaries outside of the core of 47 Tuc have met with mixed success. Mayor et al. (1984), using radial velocity techniques, failed to find convincing evidence for binaries among a sample of giants obtained about 5 core radii (r_c) from the cluster center. Hesser et al. (1987) found no evidence for binary stars using the color-magnitude diagram (CMD) of various regions of 47 Tuc (his innermost field was located at least $2.6r_c$ or 1′ from the center of 47 Tuc). Shara et al. (1988) failed to detect eclipsing variables among $\sim$3500 main-sequence stars with amplitudes $\gtrsim$0.2 mag, based on a CCD time series 3.5 hr in length. His field was about 7′ ($\sim 18r_c$) from the core of 47 Tuc. Kaluzny et al. (1995) succeeded in finding photometric binaries in the outer regions of 47 Tuc, and De Marchi & Paresce (1995) found evidence for binaries in their CMD, using the post-COSTAR Wide Field Planetary Camera (WFPC2). Their field was located $12r_c$ from the core of 47 Tuc, and their measured binary fraction was $\gtrsim$5% in the range $19 < m_{814} < 21$.

We present results based on *HST* Planetary Camera (PC) images (pre-COSTAR), which greatly extend the early searches for binaries summarized above by providing differential time series photometry, in the *U* band (F336W), of some 20,000 stars in a 66″ × 66″ field *centered on the core of 47 Tuc*. The preliminary analysis of this data set and some early results are given in Gilliland et al. (1995, hereafter Paper I). With photon noise–limited time series, characterized by an exposure length of 1000 s and continuous observing over 38.5 hr, we have detected close binary systems, such as W Ursae Majoris stars and Algols, among the BSS and upper main-sequence stars in 47 Tuc. Searches are also made for bright CVs showing intensity changes caused by orbital modulation.

One of the primary goals of this work is to arrive at an estimate of the contact binary frequency for the core of 47 Tuc, since this value is closely related to the issues of binary formation and destruction in GCs. At present, we have reasonable estimates of the overall binary frequency in the halo and disk populations and in the low-density GCs. A large amount of work based on both photometry (Carney 1983) and radial velocity studies (Stryker et al. 1985; Abt & Willmarth 1987; Carney & Latham 1987; Latham et al. 1988) implies that the binary frequency of stars in the halo is at least 20%. It is reasonable to believe that GCs, also belonging to the halo population, began with a similar fraction of binaries (Leonard 1989), and, indeed, early work on binaries in relatively low-density GCs suggests that the binary fraction is 20%–35% (Hut et al. 1992). This result has recently been supported by Yan & Mateo (1994), who assume a contact binary lifetime of 1 Gyr and estimate that the primordial binary frequency in M71 is either 22^{+26}_{-12}%, for a "flat" distribution ($df/d \log P = \text{const}$, where f is the binary frequency and P the orbital period), or 57^{+15}_{-8}%, if $df/d \log P = 0.032 \log P + \text{const}$, as observed for G-dwarf binaries in the solar neighborhood (Duquennoy & Mayor 1991). Yan & Mateo (1994) also point out that these frequencies are consistent with those of the red giant binaries detected by Pryor (see Hut et al. 1992). A similar result has been found for M5 by Yan & Reid (1996), who adopt a flat period distribution and a contact binary lifetime of 3 Gyr in order to estimate a primordial binary frequency of $28^{+11}_{-5.8}$% in this cluster, for the period range 2.5 days to 550 yr.

A second major goal of this work is to determine whether the properties of the detected binaries are consistent with the two main predictions described by Hut et al. (1992). We determine whether the binaries are more centrally concentrated than the overall stellar population and the BSS found in this study (the BSS themselves are described in detail in Guhathakurta, Edmonds, & Gilliland 1996). We also discuss whether the binaries found in 47 Tuc are likely to be primordial. A discussion of variability among the sample of BSS will be given in a separate paper (Edmonds & Gilliland 1996b).

Another goal of this paper is to search for orbital modulation of candidate CV systems. The theory of two-body tidal capture, originally proposed as the formation mechanism for low-mass X-ray binaries (LMXBs) in clusters (e.g., Fabian, Pringle, & Rees 1975; Press & Teukolsky 1977), predicts the presence of dozens of CVs in the core of dense clusters like 47 Tuc (e.g., Di Stefano & Rappaport 1994). Consequently, the almost complete dearth of dwarf novae in GCs is a recognized problem in stellar astrophysics (e.g., Shara et al. 1995; Livio 1995). Livio (1995) has suggested two possible solutions to this problem: (1) the total number of CVs in GCs is smaller than expected theoretically, or (2) the total number of CVs agrees with theory, but most of these CVs are magnetic CVs or nova-like variables and therefore do not undergo dwarf nova outbursts. Support for the second hypothesis has recently been found by Grindlay et al. (1995), who have used *HST* to show the presence of strong Hα lines in the spectra of three UV-bright stars (Cool 1993) in the dense GC NGC 6397. These stars also lie near X-ray sources (Cool et al. 1995). The properties of these stars are fully consistent with those of DQ Herculis (intermediate polar) systems.

The 47 Tuc data set and its reduction are described in § 2, with particular attention devoted to power spectrum analysis of the F336W time series. Section 3 presents the results, giving details of the variable stars detected and their classification (mostly eclipsing binaries), and giving the results of a search for CVs in the F336W time series. The section concludes with a comparison of the variable star positions with the X-ray sources detected by Hasinger et al. (1994). Evidence is presented that the two faintest eclipsing binaries may be either neutron star binaries or magnetic CVs. The results and their interpretation are discussed in § 4, where we focus on (1) the radial distribution of the binaries and (2) the consistency of the period distribution and contact binary frequency with theories for the formation of contact binaries. We conclude in § 5 by outlining the prospects for studies of binaries in GCs.

2. OBSERVATIONS AND DATA REDUCTIONS

The preliminary analysis of this data set has been described in detail in Paper I. In particular, Gilliland et al.

(1995) explains the procedure used to remove cosmic rays from the CCD images and extract intensity time series from the data. The removal of cosmic rays was complicated by x-y motion of the PC detectors relative to the PC field—this motion consisted of a sinusoidal component caused by the *HST* orbit superimposed on a low-frequency drift of ~ 1 pixel in the x-direction and ~ 0.1 pixel in the y-direction. Defects in the CCD images and the flat fields caused artifacts of this motion to appear in intensity time series extracted from the data. Despite these complications, robust elimination of cosmic rays was possible given the 99 time series frames, and time series artifacts were rare and recognizable. Paper I gives several examples of these artifacts and then gives an overview of the time series properties of a subset of 50 stars found on PC6. It also describes several classes of variable stars found in this study. Our attention now moves to the full sample of some 20,000 stars found in the PC data, beginning with a description of the search procedures used to detect variable stars.

2.1. *Data Reduction*

The reduction steps used to search for variable stars were as follows: (1) detection of the stars using DAOPHOT (Stetson 1987), (2) extraction of the intensity time series using aperture photometry and PSF fitting, (3) searching for variables using power spectrum techniques, and (4) searching for nonperiodic variability by comparing the measured rms with the expected rms of the time series.

As described in Paper I, a master list of stars and their positions was created using the mean F336W image oversampled by a factor of 2. The detection threshold of DAOFIND was set at a low level ($\sigma = 2$) in order to maximize the number of stars detected, at the expense of including some noise peaks and PSF artifacts around bright stars.

Since each CCD frame contains thousands of stars and the spherical aberration halos of each star covers a disk some 5″ wide, a false sky background is present in the data, ranging from $\sim 40e^-$ in regions at which the stellar density is the lowest to $\sim 240e^-$ near the cluster center (Paper I). This local sky is much greater than the "real" sky, which, in Paper I, was estimated to have a value of $\sim 0.7e^-$.

Before attempting to estimate the local sky for each star, a small, variable, but spatially uniform sky component was subtracted from the individual time series frames (Paper I). Then we estimated the local sky component for each star on the individual frames by matching the ratio of encircled energies at radii of 2, 3, and 4 pixels to the expected curves of growth for the PSF. This local sky estimate was then averaged over the full time series, giving us our best estimate of the local sky. An assumption of sky time invariance is perfectly appropriate for time series work (Paper I).

Intensity time series were then extracted using aperture photometry and PSF fitting by following the image motion in the manner described in Paper I. For any given stellar intensity estimate, the (x, y) position is known, as is the sky background—this allows just a one-parameter determination, providing greater accuracy than if position had to be solved for in individual cases. Stars for which the average intensity was negative were at this stage removed from the analysis. This reduction step reduced the original list of 11,590 stars on PC6 down to 7050 stars, and it removed a large fraction of the noise spikes that were detected using DAOFIND (for PC5, PC7, and PC8 this reduction step reduced the number of stars from 10,135 to 5633, 12,032 to 5899, and 7243 to 4476, respectively). However, some real stars would also have been removed with this analysis step. If we assume that the 1 σ uncertainty in the local sky estimate is $\sim 20\%$ near the core of 47 Tuc, we estimate that 0.7% of the stars with $U < 21$ will have negative intensities (16% and 34% for the $U < 22$ and $U < 23$ stars, respectively).

Two further filtering processes were applied to the star lists. First, all stars lying within 4 pixels of the edge of the CCD or the pyramid shadow were removed. Second, we attempted to remove artifacts associated with bright nearby stars. A comparison was made between the F336W magnitude of the star calculated using a sky radius of 2 pixels with the magnitude calculated using a sky radius of 4 pixels. Nearly all of the stars having a magnitude difference greater than 0.25 mag and with $U > 17$ were found, by visual examination, to be PSF artifacts around bright stars (e.g., two overlapping PSF tendrils), and these stars were eliminated from further analysis. These two steps reduced the number of stars in the star lists to 4993, 6501, 5321, and 3966 for the four CCDs, respectively (the resulting list of stars will be referred to as the "cleaned" star list). PSF artifacts will, of course, still remain in the data set—this is acceptable in a variable star search since these artifacts are not expected to show coherent oscillations apart from the signal caused by the *HST* orbit. Time series affected in this way are easily discovered using power spectrum analysis.

2.2. *Time Series rms*

To estimate how closely we approach the sensitivity limits set by Poisson noise, we have calculated the expected rms for each time series based on a noise model for aperture photometry (see Kjeldsen & Frandsen 1992). This noise model assumes Poisson noise from the counts in the aperture and the local sky, and it includes readout noise. For each CCD, calculations have been made of the ratio between the measured rms of the time series and the expected rms of the time series. Figure 1 shows, for the aperture photometry and overall magnitude ranges, the average of this ratio for the four CCDs as a function of distance from the cluster center. (The calculations have used the smaller set of stars used in the color calculations [see § 2.5] to minimize errors from near neighbors.) There are two trends with distance from the cluster center: (1) a slight decrease in noise with increasing radial distance, caused by crowding, and (2) an approximate U-shape in the curve for PC7, probably caused by errors in the flat field near the edge of PC7. The corresponding curves for the PSF fitting have a form almost identical to those for the aperture photometry, except that the average is slightly lower. When averaged over distance, the mean ratios for aperture photometry are 1.00, 1.24, 1.21, and 0.87 for the four CCDs, in turn, and, for PSF fitting, 0.92, 1.15, 1.13, and 0.81. The slight improvement from using PSF fitting is expected because (1) PSF fitting does a better job of accounting for PSF tendrils in the local sky, and (2) for faint stars, the weighting scheme will minimize the contribution from readout noise and sky noise.

The offsets between the results for the different CCDs appear to be a real property of the hardware and/or the initial data calibration used, since they occur for both measurement techniques. Further evidence can be found by considering the rms of the time series in counts (where the rms is normalized by the number of counts in the aperture)

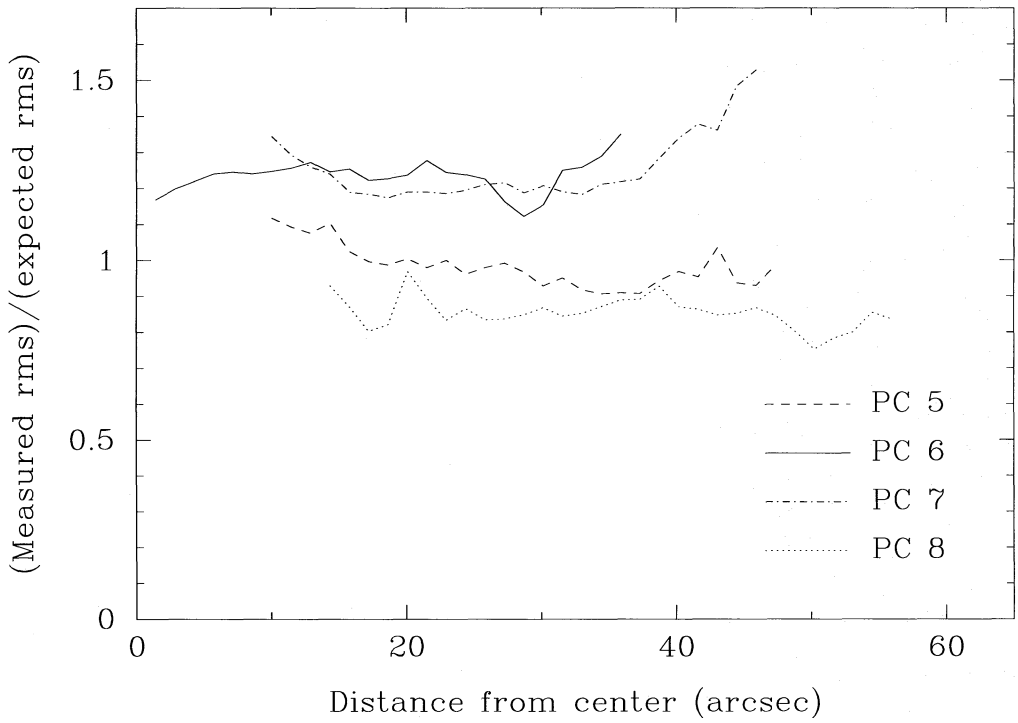

FIG. 1.—Average ratio between the measured rms of the time series and the expected rms (see text) for the four PC CCDs, as a function of distance from the cluster center.

as a function of the F336W magnitude of the stars, estimated using aperture photometry. The spread in rms values around the average value, at a given magnitude, is significantly broader for all four chips than for any single PC. If we divide the rms values by the average ratio of the measured to expected rms for the CCD in question (using the data from Fig. 1), we find a much smaller spread in rms values, only slightly larger than the typical spread for a single PC. These results confirm that there are small but significant differences between the sensitivity of each CCD chip to detecting oscillations, consistent with the ratios plotted in Figure 1. Breathing focus changes or the flat that was used for the calibration may be responsible for these differences.

2.3. *Power Spectrum Analysis*

The Lomb-Scargle periodogram (Scargle 1982; Horne & Baliunas 1986; Press & Teukolsky 1988) was applied to the time series in order to generate power spectra and to search for variables in the data set. The Lomb-Scargle method is well suited to analysis of this time series because (in increasing order of importance): (1) there are no significant gaps in the time series, (2) the time series is not evenly sampled, and (3) it gives a robust estimate of the statistical significance of any peaks in the power spectrum, providing an efficient and powerful method of searching the 20,000 stars for variability. The relevant quantity for significance is the false alarm probability (FAP; Scargle 1982), giving the probability that a peak in the power spectrum would have been produced by Gaussian noise.

The uneven spacing of the exposures means that detections of oscillations are possible at frequencies much higher than the average Nyquist frequency, as defined by Press & Teukolsky (1988), of 0.357 mHz. To illustrate this, a set of 50 simulations was run using single sinusoids added to Gaussian noise (signal-to-noise ratio for each point is 2). The frequencies of the 50 sinusoids were varied systematically from 0.02 mHz to 1.0 mHz in steps of 0.02 mHz. These functions were then "observed" by integrating over our exposure times and creating time series for the 50 different simulations. The power spectra of these 50 simulations are shown plotted above each other in the lower half of Figure 2, where the frequency of the simulations increases from bottom to top in the figure. Clearly, the sinusoidal signal is visible in the power spectra at frequencies as high as 0.7 mHz, about twice the average Nyquist frequency. At higher frequencies, the signal decreases significantly because the average value of the oscillation over the exposure time approaches zero. Aliased peaks are also visible in the power spectra, in such a way that the true frequency and the aliased peak are centered on 0.45 mHz (the Nyquist frequency of the few 900 s exposures closest together in the time series). The average ratio between the power in the true peak and the power in the aliased peak is ~ 2.0.

To show our improved ability to measure high frequencies with our data sampling, we show in the top half of Figure 2 the corresponding simulations for evenly spaced observing times, assuming 1000 s exposure times plus overhead, and the same timespan as the observed time series. Clearly, at frequencies greater than the Nyquist frequency, there is now ambiguity in choosing the peak in the power spectrum corresponding to the input sinusoid. With no 900 s exposures, the effective Nyquist frequency is also reduced.

Guided by the above discussion, we limited our power spectrum calculations to frequencies less than twice the average Nyquist frequency, 0.714 mHz. With the exception of possible double degenerate systems, no periodic astrophysical phenomena are expected in this data set with periods shorter than the cutoff period of 23 minutes. Figure 2 shows that there will be a reduction in sensitivity at periods below ~ 1 hr. More detail of this effect is shown in Figure 3, which plots a conservative estimate of the detect-

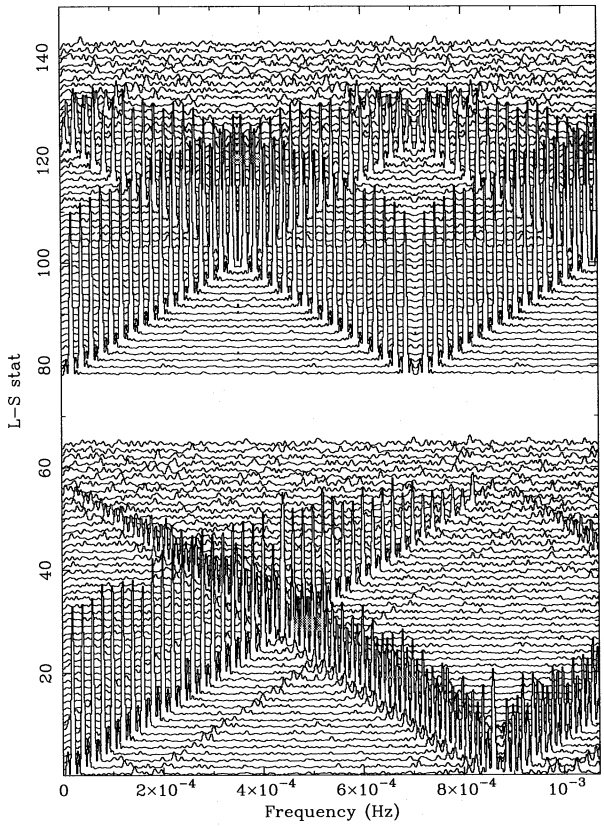

FIG. 2.—Resulting power spectra for two sets of 50 time series simulations with single sinusoids added to small amounts of Gaussian noise (S/N = 2). Frequencies of the injected sinusoids range from 0.02 to 1.0 mHz in steps of 0.02 mHz. The lower half of the figure shows the power spectra for the (unevenly spaced) 47 Tuc time series, while the top half of the figure shows the power spectra for evenly spaced time series with the same timespan as the 47 Tuc data.

able oscillation amplitude, in F336W mag units, for a single sinusoid as a function of magnitude. The detectable threshold was assumed to be an FAP less than 1×10^{-4} (see justification below). The average noise value at the given magnitude was adopted and four different input periods were used. The detectable amplitude for 0.5 hr periods is 77% higher (poorer) than that for 4 hr periods, while the detectable amplitude for 1 hr periods is only 12% higher.

2.4. *Variable Search*

When searching a large sample of power spectra for periodicity it is important to calculate how many significant peaks are expected based on Gaussian statistics alone. For this purpose, we have generated 200,000 independent time series using our sampling function and a Gaussian noise generator (Press et al. 1992), and we have calculated power spectra and the FAP of the highest peak in each power spectrum. Table 1 shows how many simulated power spectra have a peak with an FAP less than a given value. The numbers for the 200,000 simulations in Table 1 have

TABLE 1

NUMBER OF SIMULATED POWER SPECTRA WITH AN FAP LESS THAN A GIVEN VALUE

FAP	Power Spectra
1.00	20781
0.50	9514
0.10	1616
0.05	746.4
0.01	117.6
5×10^{-3}	48.21
1×10^{-3}	7.585
5×10^{-4}	2.286
1×10^{-4}	0.5195
5×10^{-5}	0.2078

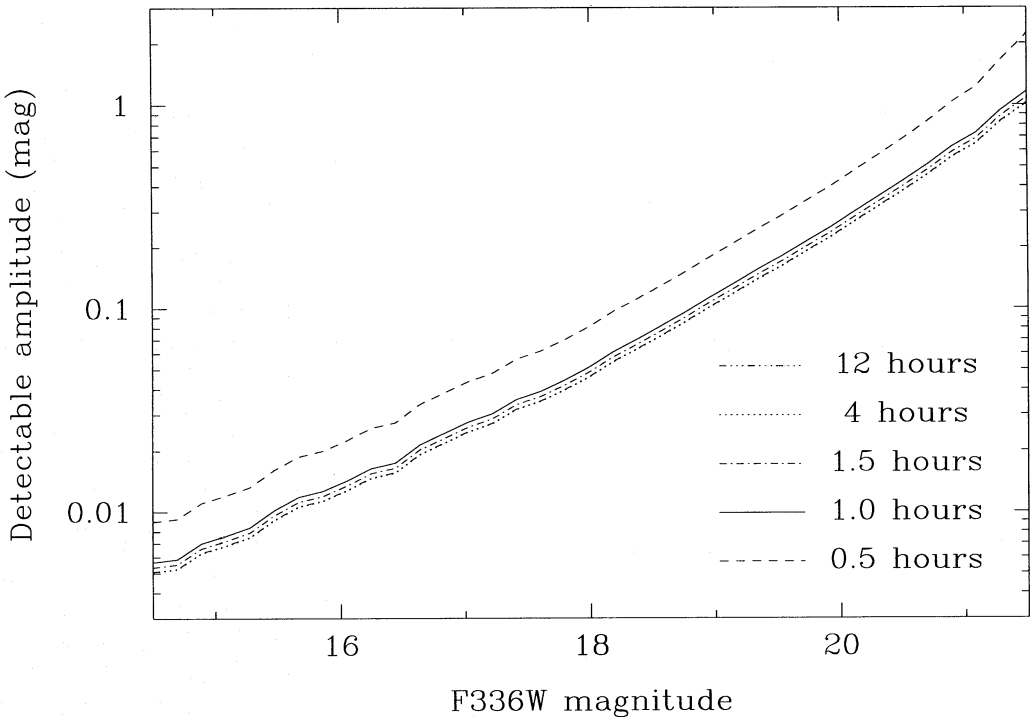

FIG. 3.—Detectable oscillation amplitude (in F336W magnitude units) for a single sinusoid with five different input periods as a function of magnitude. The average noise value at the given magnitude has been adopted.

been normalized to 20,781, the number of power spectra in our sample.

Guided by these numbers, searches were made for stars having peaks in their power spectrum with an FAP less than 1×10^{-4} in each of the aperture and PSF fitting photometry. Based on our Gaussian noise simulations, only 0.51 time series in a total of 20,781 are expected to have an FAP this small. A second constraint was that, for each star, the respective peaks in the power spectra from the aperture and PSF fitting photometry should differ in frequency by less than twice the frequency resolution of the power spectra.

Besides avoiding periodicities generated by noise, use of this threshold minimized the detection of two types of artifacts found in this data set, low-frequency variability and intensity changes at the orbital frequency of the *HST* (Paper I gives several examples). Both of these are caused by image defects, such as stars lying near bad columns or stars with bright neighbors, interacting with the small x-y image motion.

2.4.1. *High Frequency*

Several techniques were used to avoid the low-frequency variability caused by near neighbors and image defects: (1) the search was made for variables with periods less than 15 hr; (2) the search for peaks in the power spectrum avoided periods within 1 minute of the *HST* orbital period and twice this period; and (3) to filter out time series severely affected by the *HST* orbit, power spectrum peaks having an FAP less than 0.01 within 1 minute of the *HST* orbit, and twice this period were automatically removed from the analysis (for the PC6 aperture photometry, for example, 253 time series out of 7050 were removed using these constraints).

2.4.2. *Low Frequency*

A similar technique was used to search for variables with periods longer than 15 hr, but at these lower frequencies the time series of apparently variable stars were dominated by errors in the photometry, mainly caused by near-neighbor effects. The signal detection threshold was therefore raised by lowering the FAP upper limit to 1×10^{-6}, resulting in 60–100 detections per CCD. The near neighbors were examined by plotting, for each candidate variable, the distance to the nearest neighbor and its relative magnitude, resulting in a list of some 40 stars apparently unaffected by bright near neighbors.

2.4.3. *Nonperiodic Phenomena*

A search was also made for stars having rms variations considerably greater than that expected from simple noise statistics for aperture photometry (using the model explained earlier). All stars having the ratio of the measured to expected noise greater than 2 and with no near neighbors were singled out for close examination. This analysis recovered the higher amplitude variables already discovered using power spectrum techniques and some of the low-frequency variability caused by image defects such as bad columns.

A handful of other candidate variables with unusually high rms were found. In several of these cases, the apparent variability was again low-frequency changes caused by coupling of image defects with the x-y motion of *HST*. In three cases, the variability arose completely from a faulty pixel or pair of pixels giving a highly erratic signal as a function of time. This behavior was easily confirmed by examining the time series contribution from individual pixels as a function of time. No believable candidates were found using this search technique.

2.5. *Color Measurements*

To provide color information for the stars, additional F439W and F555W exposures (approximating B and V) were taken of 47 Tuc using the same pointing as for the F336W time series (Paper I). Since these data are affected by spherical aberration, Guhathakurta et al. (1996) has estimated instrumental U, B, and V magnitudes by modeling in detail the core and extended wings of the *HST* PSF as a function of CCD position. The final list of stars with measured colors for the four CCDs contained 14,801 stars, after special care was taken to exclude PSF artifacts and CCD blemishes. The instrumental magnitudes were then transformed to Johnson UBV magnitudes by comparing with the photometry published by Aurière, Lauzeral, & Koch-Miramond (1994). Full details are given in Guhathakurta et al. (1996).

3. RESULTS

3.1. *Overview of Discovered Variables*

The high-frequency (period <15 hr) discovery criteria enabled 11 variable stars to be detected, eight of them on PC6, and one each on PC5, PC7, and PC8. Only two of the ~ 40 candidate variables found with the low-frequency search are obviously bona fide variables because of their large amplitude or distinctive light curve, one of them on PC6 and one on PC8. The other candidate variables are mostly giant stars and have low-frequency, low-amplitude signal not easily explained by errors or artifacts. One or two of these may be Mira or semiregular variables having periods much longer than 40 hr, but many of the others appear to represent a new type of variability in 47 Tuc; these candidate variables will be discussed in Edmonds & Gilliland (1996a).

Summaries of the 13 variables discovered in 47 Tuc are given in Tables 2 and 3. In Table 2, column (1) lists the number we have assigned to the variable; column (2) lists which CCD the variable falls on (5)–(8); columns (3) and (4) list the offset, in arcseconds, of the variable from star E in Guhathakurta et al. (1992); column (5) lists the distance (r_v) of the variable from the center of 47 Tuc (as defined by Guhathakurta et al. 1992); column (6) lists the FAP of the peak in the power spectrum for the aperture photometry; column (7) the corresponding FAP for the PSF fitting; and column (8) gives the ratio of the measured to expected rms, for aperture photometry, normalized by the average value of this ratio (these will be referred to as normalized rms values, rms_n). To show the significance of the numbers in column (8), we have calculated the average of the normalized rms values for the four CCDs: PC5, 0.97 ± 0.13; PC6, 1.00 ± 0.10; PC7, 1.01 ± 0.13; and PC8, 0.98 ± 0.15. For this calculation, we avoided variable stars and stars having their signal heavily influenced by bright near neighbors by removing objects having a normalized rms greater than 2, explaining why the average normalized rms values are generally different from 1.0. This procedure removed only 16, 10, one, and nine stars from the data for the four CCDs in turn, but removed several data points with very large rms values. Column (9) gives the period of the variable in days,

TABLE 2

POSITIONS AND LIGHT-CURVE PROPERTIES OF 47 TUC VARIABLES

ID	PC	δx[a] (″)	δy[a] (″)	r_v (″)	FAP of Power Spectrum Peak (Aper phot)	FAP of Power Spectrum Peak (PSF Fitting)	rms_n	Period (days)	Amp (mag)	Type
1.....	5	5.65	16.88	13.94	5.50(−17)	5.36(−17)	6.71	0.0636	0.177	SX
2.....	6	17.95	−10.89	20.98	8.05(−10)	1.08(−09)	6.82	0.1019	0.135	SX
3.....	6	6.53	3.94	4.08	1.48(−13)	1.03(−12)	2.82	0.0558	0.091	SX
4.....	6	12.33	−4.12	12.32	1.57(−15)	6.00(−16)	2.18	0.330	0.358	EW
5.....	6	22.47	2.32	19.99	9.47(−09)	1.86(−10)	1.39	0.146[b]	0.216	EW/NL(?)
6.....	6	2.10	0.36	2.97	1.13(−15)	7.28(−15)	2.28	0.558	0.085	EW
7.....	6	0.56	2.88	1.94	7.60(−05)	3.76(−05)	1.31	0.414	1.73	EA(?)
8.....	7	−7.74	−10.72	17.32	3.61(−05)	1.51(−06)	1.13	0.514	0.49	EA(?)
9.....	5	−8.81	27.65	26.85	2.18(−14)	1.45(−14)	2.23	1.5	0.419	EB
10.....	6	12.84	−7.69	15.09	8.60(−12)	1.50(−11)	4.39	0.428	0.439	EB
11.....	6	−0.85	−1.07	5.51	1.86(−09)	1.80(−09)	4.36	1.16	1.2	EA
12.....	6	6.21	8.80	6.64	1.05(−05)	1.01(−06)	1.48	0.69[c]	0.060	?
13.....	8	−17.20	6.44	19.94	2.39(−06)	3.19(−06)	8.01	0.97	1.65	EA

[a] With respect to star E in Guhathakurta et al. 1992.
[b] Period could also be 0.329 days.
[c] Period could also be 1.38 days.

column (10) gives the peak-to-peak amplitude of the variable in F336W magnitude units, and column (11) lists the variable type, using the nomenclature of the General Catalogue of Variable Stars (GCVS; Khopolov et al. 1985).

Figure 4 shows the time series standard deviations of all cleaned stars plotted against instrumental F336W ($\approx U$) magnitude, with the normalization explained in § 2.2. Symbols are plotted for the 13 variables found in 47 Tuc.

Table 3 lists the color information for each of the variable stars, where only instrumental F336W magnitudes are available for the fainter variables 7 and 8. The U magnitudes quoted are based either on the average oversampled image, representing the magnitude averaged over the time series for the pulsating variables (1–3), or the maximum magnitude for the binary candidates (4–13). The B and V magnitudes were corrected to the mean or maximum intensity, and the $V-I$ colors were obtained from Guhathakurta et al. (1992).

The systematic uncertainties (e.g., from PSF template errors and crowding) for the UBV photometry were estimated by computing the rms along the giant branch in each of U versus $U-B$, B versus $U-V$, and V versus $B-V$. We assumed zero intrinsic width for the RGB, so these uncertainties are formally upper limits. To compare our colors with those of other work, the total absolute uncertainty in the colors for an individual star will be a combination of the systematic and external uncertainties and the generally small contributions from Poisson noise and readout noise, all added in quadrature. The external uncertainties (equivalent to uncertainties in the zero point of the time sequence) include sources of absolute uncertainty, such as filter transmission uncertainties—we conservatively estimate the external uncertainty to be twice the systematic uncertainty. Table 3 shows the magnitude and color uncertainties for each of the variable stars. The photon noise component starts to make a noticeable contribution to the noise budget for variables 5 and 8, and dominates the uncertainty for variable 7.

Light curves for the binary candidates are shown by Figures 5 (variables 4–8) and 6 (variables 9–13), and power spectra are shown by Figures 7 and 8. Variables 1–6 and 9–11 are all obvious variables because of the small values of the FAP and the large values of the normalized rms. Variable 7 has a value of the FAP only marginally smaller than the threshold determined by the noise simulations, but it has an rms value at the 3 σ level and so is considered a firm variable. Variable 8 has a lower amplitude than variable 7

TABLE 3

COLORS OF 47 TUC VARIABLES

ID	U	$U-B$	$B-V$	$V-I$	$\sigma(U)$	$\sigma(U-B)$	$\sigma(B-V)$
1.....	15.98	−0.06	0.48	0.54	0.23	0.31	0.23
2.....	15.78	0.14	0.42	...	0.23	0.31	0.23
3.....	16.13	−0.31	0.31	0.46	0.23	0.31	0.23
4.....	17.89	−0.40	0.82	0.16	0.23	0.32	0.24
5.....	18.72	−0.60	1.67	0.94	0.24	0.34	0.25
6.....	15.91	−0.22	0.27	0.47	0.23	0.31	0.23
7.....	19.92	...	...	...	0.53	...	...
8.....	19.14	...	...	...	0.27	...	...
9.....	17.93	−0.39	0.90	...	0.23	0.32	0.24
10.....	16.95	−0.36	0.64	0.60	0.23	0.31	0.23
11.....	17.66	−0.43	1.06	...	0.23	0.32	0.24
12.....	16.41	−0.23	0.68	...	0.23	0.31	0.23
13.....	17.91	0.01	0.71	...	0.24	0.32	0.24

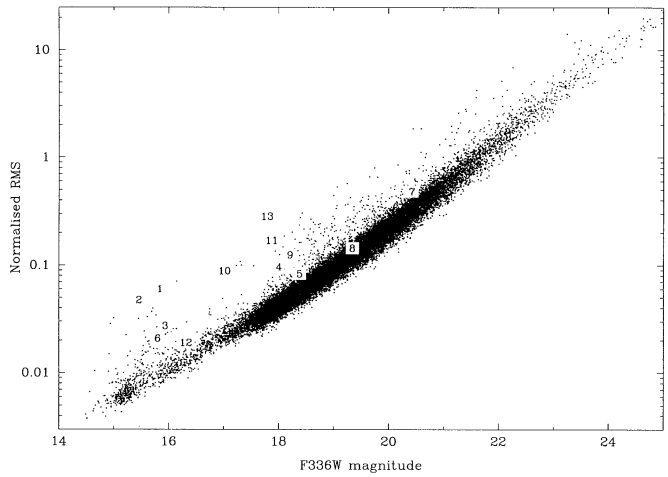

FIG. 4.—Time series standard deviations of all 20,781 stars plotted against F336W ($\approx U$) magnitude. We have divided the rms by the average ratio of the measured to expected rms for the CCD in question, using the results from Fig. 1.

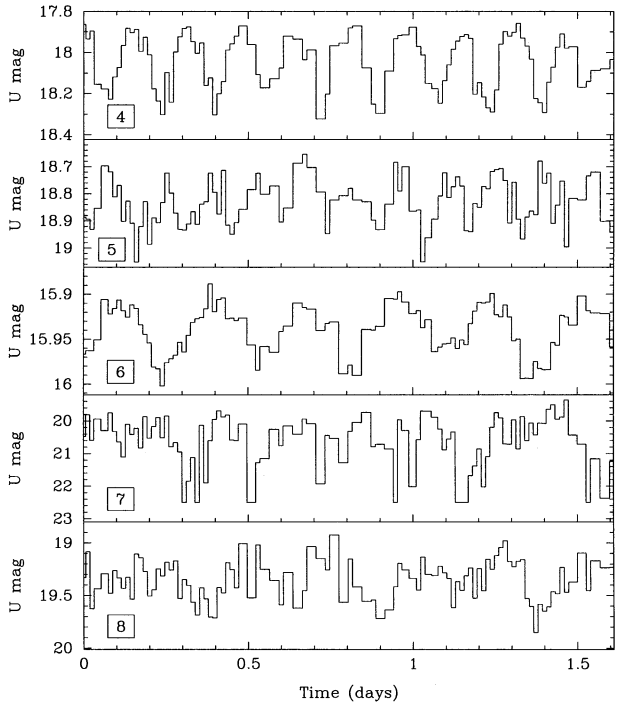

FIG. 5.—Light curves for variables 4–8

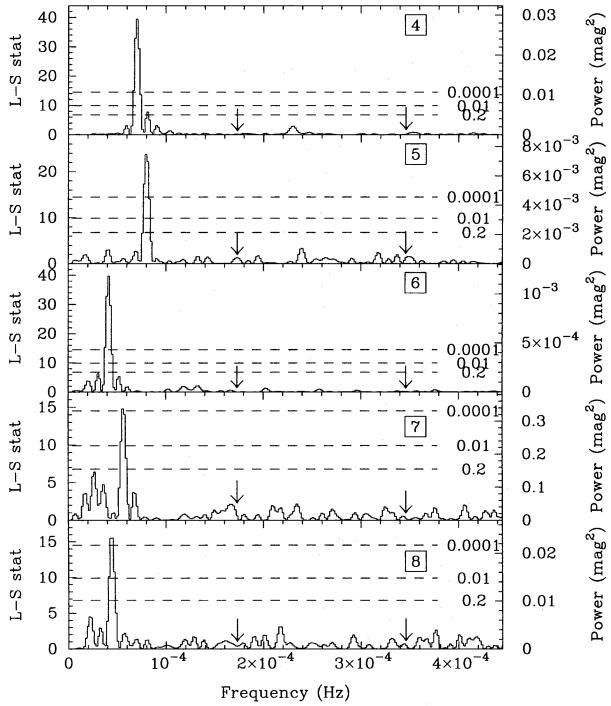

FIG. 7.—Power spectra for variables 4–8 (note that the highest frequencies are not plotted). Arrows show the orbital frequency of *HST* and twice this frequency.

and therefore a smaller normalized rms (1.0 σ), but the FAP, particularly for the PSF fitting results, is still significant. The rms value for variable 12 is 4.6 σ away from the average, implying the intensity is certainly varying, although part of the long period signal may be caused by an artifact of the *HST* motion. Variable 13 has a large rms value but a less significant FAP, since the signal in the power spectrum is spread out over multiple peaks.

3.1.1. *Test of Variability Using Chi-Squared Map*

An additional test of the variability of a source is to examine the corresponding position in the chi-squared map (for details, see Paper I). This technique was not used as a primary tool in searching for variable stars, since many artifacts appear in the chi-squared map. Most of the variable stars discussed here show obvious stellar-like objects in the chi-squared map within 1 pixel of the stars' position.

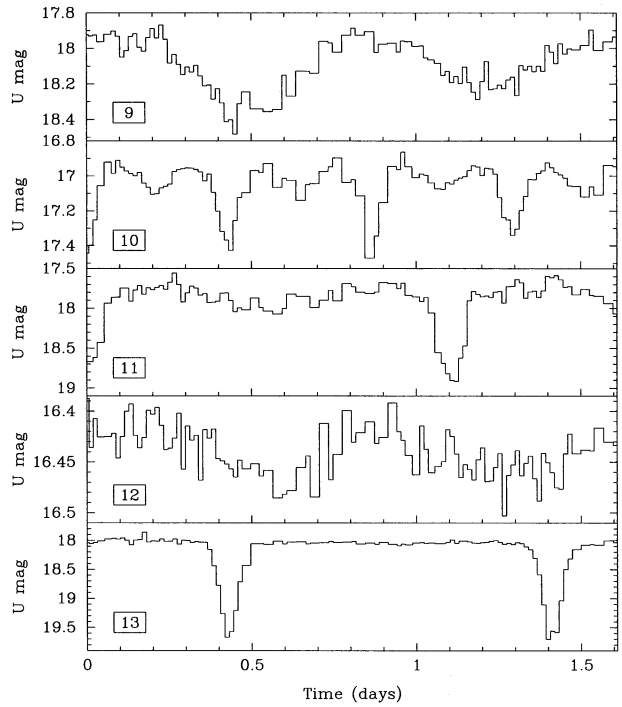

FIG. 6.—Light curves for variables 9–13

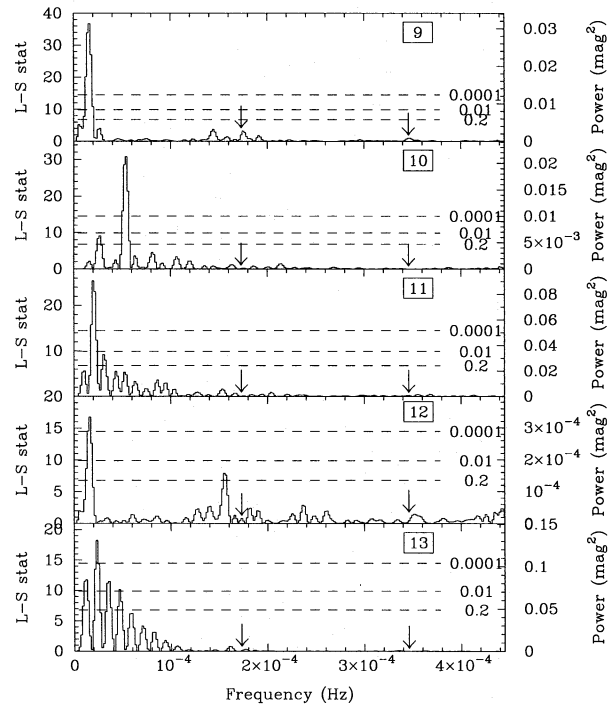

FIG. 8.—Power spectra for variables 9–13

For example, for PC5, variable 1 has a source in the chi-squared map with S/N ratio greater than 10 (50 objects found with S/N > 10 over the whole PC image), while variable 9 has a S/N between 5 and 10 (221 objects found with S/N ratio in this range). For PC6, variables 2, 4, 10, and 11 all have S/N > 10 (13 objects with S/N > 10), variable 6 has 5 < S/N < 10 (106 found), variable 5 and variable 3 have 3 < S/N < 5 (1741 found), and variable 7 has 2 < S/N < 3 (7778 found). For PC8, variable 13 has S/N > 10 (60 found). No object was found in the chi-squared map for PC7 at the position of variable 8, which is not surprising because of its low amplitude and relative faintness.

3.2. *Membership of 47 Tuc*

There is only a very small chance that any of the variable stars found are foreground or background objects because of the small PC field of view and the high Galactic latitude of 47 Tuc. There are two main potential sources of contamination for stars lying in our PC field. First, there is the possibility of field stars. Using the models of Ratnatunga & Bahcall (1985), we estimate a total of 0.57 stars in our field brighter than $V = 19$, and 1.38 stars brighter than $V = 21$. There will be a second contribution from the SMC, which lies 4° away from 47 Tuc. Using the estimates of Hesser et al. (1987) within a box ($0.0 < B-V < 0.8$; $21 < V < 24$) enclosing the bulk of the SMC turnoff region but none of the 47 Tuc main sequence, around 33 stars are expected in our field. Therefore, we expect only around two or three stars in our field with $V < 19$ (~0.5 mag brighter than the SMC horizontal branch) and, at most, around five with $V < 21$.

3.3. *Variable Star Classification*

The periods and amplitudes of the variable stars, as well as their light curves and positions in the CMD, provide important clues in classifying their variability. The variable stars 1, 2, and 3 are all BSS (see the CMD shown by Fig. 10), and their short periods and small amplitudes imply they are undergoing SX Phe–type pulsations. These stars will be analyzed in detail by Edmonds & Gilliland (1996b).

As an aid in interpreting the light curves of the W UMa candidates, variables 4–8, phase plots were calculated (setting phase = 0 to be the primary minimum in the phased light curve) and fits of the form $l(\theta) = \Sigma_0^{11} a_i \cos(2\pi i\theta)$ were made to these phase plots. This functional form is used because of its simplicity and its relevance to fitting W UMa light curves (see Rucinski 1993). Figure 9 shows the phase plots and fits for variables 4–8, where we have assumed that the period is twice that calculated from the peak in the power spectrum.

The sinusoidal nature of the light curve for variable 4, its position in the CMD near the main-sequence turnoff, and its period and amplitude imply that it is probably a W UMa star. Note from the fit to the light curve that the eclipses are sharper than the turning points in the light curve at phases 0.25 and 0.75, as expected for a W UMa star (see, e.g., the fits in Yan & Mateo 1994).

The next variable, 5, is too faint to be a SX Phe variable, but the classification of it as a contact binary is problematic since no consistent position in the CMD can be discerned from plotting V versus $B-V$, B versus $U-B$, and U versus $U-V$ (see Fig. 10). The V versus $B-V$ and U versus $U-V$ plots imply that variable 5 lies redward of the main sequence (by ~0.9 mag and ~0.5 mag, respectively), just

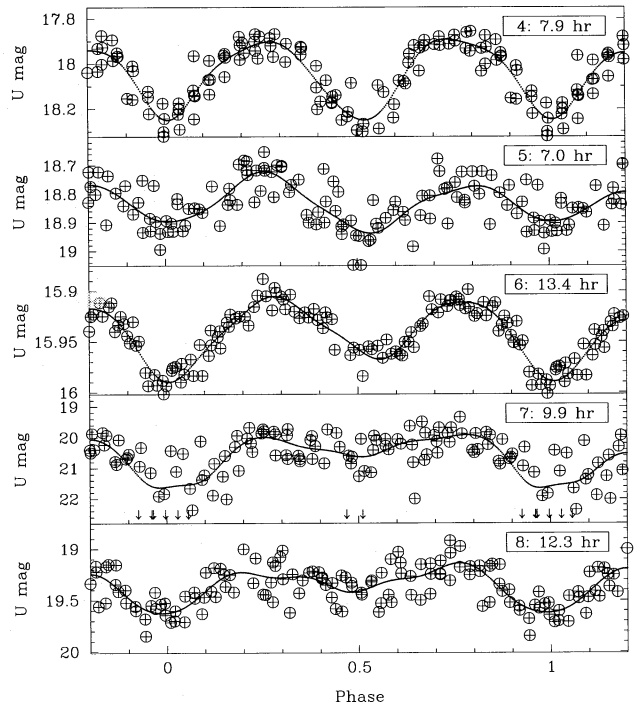

FIG. 9.—Phase plots and fits (see text) for variables 4–8. Adopted period for each variable is shown, and arrows show where variable 7 is fainter than $U = 22.5$.

below the turnoff, but the B versus $U-B$ plot implies that the star lies to the blue side of the main sequence, by ~0.3 mag [the total systematic uncertainties for variable 5, including Poisson noise, are 0.19 mag ($U-B$), 0.14 mag ($B-V$), and 0.14 mag ($U-V$)]. These results imply that, compared to the other variable stars, variable 5 is unusually bright in the V band if it is a W UMa star. This behavior is inconsistent with the expected properties of a W UMa system. A $V-I$ color is also available for variable 5, but since it lies near the detection limit in the data set of Guhathakurta et al. (1992), the uncertainty is large. There is a suggestion of differences between the heights of the two peaks and the depths of the two eclipses in Figure 9, but this difference is marginal with our limited signal-to-noise ratio.

In a crowded field such as this, there is the possibility of contamination from a red main-sequence star close to the line of sight of variable 5. The nearest neighbor to variable 5 is a relatively bright star (0.75 mag brighter than variable 5), but it lies at the base of the main-sequence turnoff in all three of the CMDs listed above and, therefore, has "normal" colors. A contaminating star could also lie along the same line of sight as variable 5, but there is a very small chance that such a star would be red enough and bright enough to significantly change the colors of variable 5.

It is interesting to note that two of the W UMas found by Yan & Mateo (1994) lie to the red of the main sequence, one by a considerable margin. Yan & Mateo (1994) point out that similar red binaries have been found in open clusters NGC 188 (Kaluzny, Mazur, & Krzeminski 1993) and Be 39 (Kaluzny et al. 1993) and the globular cluster NGC 4372 (Kaluzny & Krzeminski 1993). Since no U data is available for any of these systems, a direct comparison with variable 5 is not possible (see § 3.3.1 for more discussion).

The variable 6 is a BSS with a distinctive W UMa–type light curve (although the difference between the primary

and secondary minima are larger than for most W UMa stars). Its period is also consistent with a W UMa variable, and the small amplitude suggests a low-inclination angle. An interesting feature of the light curve is the apparent discontinuities near phases −0.05 and 0.45, perhaps indicating spots on the surface of one of the stars. Possibly linked to this is the apparent asymmetry in the light curve, with the middle eclipse occurring near phase equal to 0.55. A rigorous analysis of these features may be attempted by full light-curve fitting to these phase plots.

Variable stars 7 and 8 have much smaller signal-to-noise ratios, but both appear to have light curves of the β Lyrae or Algol type. The difference in eclipse depths probably discounts W UMa–type systems. Unfortunately, the stars are too faint for useful magnitudes to have been estimated from the B and V images. More discussion of these two interesting variables will be given in §§ 3.4 and 3.6.

The variable stars 9, 10, 11, and 13 are all eclipsing variables located near the main-sequence turnoff. The smoothly changing light curve of variable 9 implies that the binary system is in contact. However, the period of the system, around 1.5 days, is longer than most known W UMa stars, and the difference between the eclipse depths for the primary and secondary is also larger than expected for W UMa systems. Therefore, we classify this star as an eclipsing variable of the β Lyrae type. The light curve and period of variables 10 and 11 imply that they are β Lyrae and Algol eclipsing binaries, respectively (note from Figs. 7 and 8 that there is power at half the frequency of the power spectrum peak for variables 7, 9, 10, and, to a lesser extent, variable 8, related to the difference in eclipse depths between the primary and secondary minima). The variable 13 is probably an Algol, and it is interesting because there appears to be no evidence for a secondary eclipse, perhaps indicating a large temperature difference between the two stars.

The variable star 12 has no obvious classification. Figure 10 shows that it is a BSS and lies close to the three SX Phe pulsators, variables 1–3, but the two periods quoted in Table 2 are unusually long for such a pulsating star. It could be a binary system, such as an ellipsoidal variable, although this would not explain the asymmetrical appearance of the light curve. Figure 8 shows evidence for a peak near 0.16 mHz, so it is possible that we have detected a low-amplitude SX Phe variable in a binary system.

3.3.1. *Light-Curve Fitting*

To assist in the identification of variables 4–8 and to attempt simple light-curve fitting, we use the light curves calculated by Rucinski (1993) for W UMa stars. Rucinski provides tables of Fourier cosine coefficients for light curves of contact binary stars for one (solar) effective temperature. These Fourier coefficients may be combined with Rucinski's depths of minima to calculate light curves for a broad range of geometrical parameters. These parameters are the orbital inclination (i, between 30° and 90°), values of the mass ratio (q, between 0.05 and 1.0), and three values of the degree of contact (f). Rucinski's calculations are applicable to a large range of effective temperatures since, as he argues, temperature has a very small influence on the shape of W UMa light curves.

For each star, the best fit to the Rucinski (1993) light curves was found by searching for the minimum residual difference between Rucinski's light curves and the measured light curve. This search was made over the full ranges in q and i, for each of the three different f values (note that the Rucinski 1993 tables have been extrapolated in order to give light curves at angles of inclination between 0° and 30°). Table 4 shows the accuracy of these fits by listing in column (5) the rms of the residual differences for variables 4–8. In column (6), we list the residuals normalized by the rms noise of the measured time series, where the rms noise is estimated by subtracting the fits described at the beginning of § 3.3. Finally, in column (7), we list the residuals normalized by both the rms noise and the rms of the light-curve modulation (the rms of the fits described at the beginning of § 3.3, which are proportional to the amplitude of the

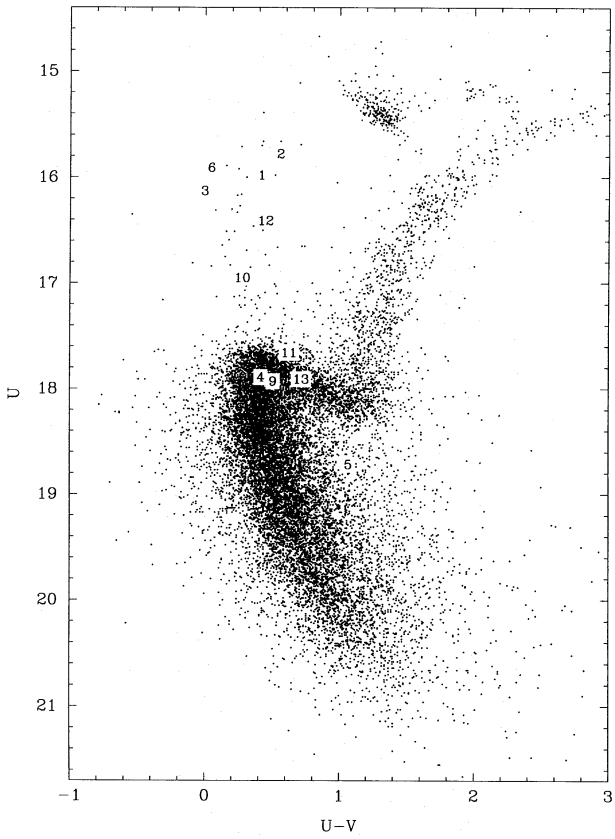

FIG. 10.—U vs. $U-V$ CMD for stars in 47 Tuc, with labels for the variable stars.

TABLE 4

RESULTS OF FITS TO W UMa CANDIDATES

ID	i	q	f	res	res / rms	res / amp × rms
4.....	90.0	0.20	1	0.057	1.132	10.7
4.....	62.5	0.90	2	0.056	1.103	10.3
4.....	52.5	0.95	3	0.057	1.124	10.6
5.....	55.0	0.95	1	0.058	1.084	19.6
5.....	42.5	0.90	2	0.058	1.090	19.9
5.....	37.5	0.65	3	0.058	1.084	19.4
6.....	35.0	0.95	1	0.015	1.653	67.2
6.....	27.5	0.75	2	0.015	1.674	68.9
6.....	25.0	0.50	3	0.014	1.651	71.8
7.....	90.0	0.95	1	0.544	1.271	3.1
7.....	90.0	0.90	2	0.539	1.259	3.1
7.....	90.0	0.75	3	0.530	1.238	3.0
8.....	87.5	0.10	1	0.156	1.245	10.2
8.....	90.0	0.10	2	0.155	1.232	10.0
8.....	90.0	0.10	3	0.153	1.218	9.9

variable). When the residuals normalized by the rms noise values are considered, we see little difference between the results, apart from a relatively poor fit for variable 6. Since there are large differences between the amplitudes of the variables in question, a more useful comparison may be the residuals normalized by both the rms noise and the rms of the variables' light curve. Column (7) shows that the light curve for variable 5 gives a poorer fit to the W UMa light curves than that for variable 4. Variable 6 gives the poorest fit, owing both to the uneven eclipse depths and to the asymmetry in the light curve discussed above. Clearly, more study of this unusual binary system would be of great interest. The fits for variables 7 and 8 are surprisingly good, but the high noise levels for both of these stars limits the usefulness of the fits.

A second important feature of Table 4 is that for any given star there are small differences between the residuals for the three different values of f. Also, for some stars, there are large variations in the values of q and i for the three different fits. For example, with variable 4, the best fit for $f = 0$ is ($i = 90$, $q = 0.2$), while for $f = 0.5$, the best fit is ($i = 62.5$, $q = 0.90$). Furthermore, even assuming a value of f, only pairs of q and i can be found—this redundancy is expected because a smaller value of either q or i, keeping the other parameter constant, decreases the amplitude of the light curve. These results show that no reasonable predictions can be made for the fundamental parameters of the light curves, f, i, and q.

An additional method can help determine whether the variables 4–6 are W UMas. Rucinski (1994) has derived calibrations for the absolute magnitudes, M_V, of contact binary systems in terms of their orbital period and color indices $B-V$ and $V-I_c$ (a modification to this calibration takes into account differences in metal abundances between clusters; Rucinski 1995). Note that, if a star is a W UMa system, then the period will correspond to double the period calculated from the peak in the power spectrum, since the light curve for a W UMa will be close to sinusoidal. This implies that there is no ambiguity in the period determination if the stars are W UMa systems.

Rucinski (1994) uses his calibration to check the likelihood of membership for W UMa stars in three low Galactic latitude clusters by comparing the expected absolute magnitude with the absolute magnitude measured assuming that the stars lie in the cluster. He uses a conservative limit of ± 1 mag (approximately $\pm 4\ \sigma$) to eliminate probable foreground or background objects. Since the chance of variables 4–6 being background or foreground objects is negligible, we can assume that these three stars all lie in 47 Tuc. Thus, large differences between the expected and measured M_V should indicate that the star in question is unlikely to be a W UMa system.

Using the values of the distance modulus (13.4) and metal abundance ([M/H] = −0.65) for 47 Tuc measured by Hesser et al. (1987), we calculated the absolute magnitude difference $\Delta M_V = M_V^{\rm obs} - M_V^{\rm pred}$, where $M_V^{\rm obs}$ is the observed absolute magnitude at maximum light and $M_V^{\rm pred}$ is the absolute magnitude predicted by Rucinski (1994, 1995). The differences using the $B-V$ calibration are −0.90 mag, −4.50 mag, 0.25 mag, 0.15 mag, 0.20 mag, and −0.71 mag, for variables 4–8 and 10, respectively. Variables 7, 8, and 10 have been included for comparison even though they are unlikely to be W UMa systems, and we have assumed main-sequence colors for variable 7 and 8. Thus, for the $B-V$ calibration, two of the candidate W UMas (variables 4 and 6) lie within the 1.0 mag uncertainty defined by Rucinski (1994). Clearly, variable 5 is the exception.

For the absolute magnitude differences of variables 4–8 and 10 to be reduced to zero, the required uncertainties in $B-V$ are −0.21, −1.06, 0.06, 0.04, 0.05, and −0.17 mag, respectively. For the difference of variable 5 to be merely reduced to 1 mag requires an uncertainty in $B-V$ of 0.82 mag, which is still considerably larger than the conservative estimates of the uncertainty given in Table 3. These results indicate that variable 5 is unlikely to be a W UMa system, in agreement with the tentative conclusions based on the CMD positions of the star and the shape of its light curve. Note that the two eclipsing binaries in M71, which lie to the red of the main sequence (Yan & Mateo 1994), both have absolute magnitude differences well within the 1.0 mag limit quoted by Rucinski (1994). This suggests that variable 5 represents a different sort of variable star to the W UMas found in M71.

The $V-I$ calibration of Rucinski (1994) implies that variable 6 is a W UMa system but that variables 4 and 5 have colors marginally inconsistent with W UMa systems. This test is probably not useful for these stars, however, because variables 4 and 5 are both close to the limiting magnitude in the data set of Guhathakurta et al. (1992) and there are large uncertainties present in the $V-I$ data.

3.4. *Comparison with Known Variable Stars*

An additional guide to the identification of the variable stars is possible by comparing their period and amplitude with the 3727 eclipsing binaries in the GCVS (Khopolov et al. 1985). Figure 11 plots period versus amplitude for the four main types of eclipsing binaries in the GCVS, using a different symbol for each. Variables 4–13 are also included in this figure. The types of eclipsing binaries defined in the GCVS are E for completely detached eclipsing binaries (*open squares* in Fig. 11), EA for Algol-type eclipsing systems in which there are periods of almost constant light between eclipses (*filled circles*), EB for β Lyrae–type eclipsing systems in which the light is changing continuously between eclipses (*open circles*), and EW for W UMa–type eclipsing binaries (*plus*). Those EA eclipsing systems that are also known to show nova-like behavior or contain the nuclei of planetary nebulae are plotted as NL and PN, respectively, using the nomenclature in the GCVS.

Eclipsing systems of the type EA are the most common type of eclipsing binary in the GCVS, with 2607 systems, most of them with periods longer than 1 day and many with amplitudes greater than 1 mag. Below periods of 1 day, EB and EW systems dominate (580 and 540 systems, respectively), most of them with amplitudes less than 1 magnitude.

Figure 11 clearly shows the unusual nature of variable 7 when compared with the other eclipsing binaries. This variable occupies a region of the plot where the only binaries with larger amplitudes and shorter periods are four Algol-type systems with nova-like light curves (three of these with known white dwarf companions) and one Algol system containing the nucleus of a planetary nebula. Searching the GCVS for other types of variables with similar period and amplitude gives several hundred RR Lyrae variables. Since variable 7 lies close to the horizontal branch in the SMC and three or four stars from the SMC are expected to lie in our field, there is a small chance that variable 7 is an RR

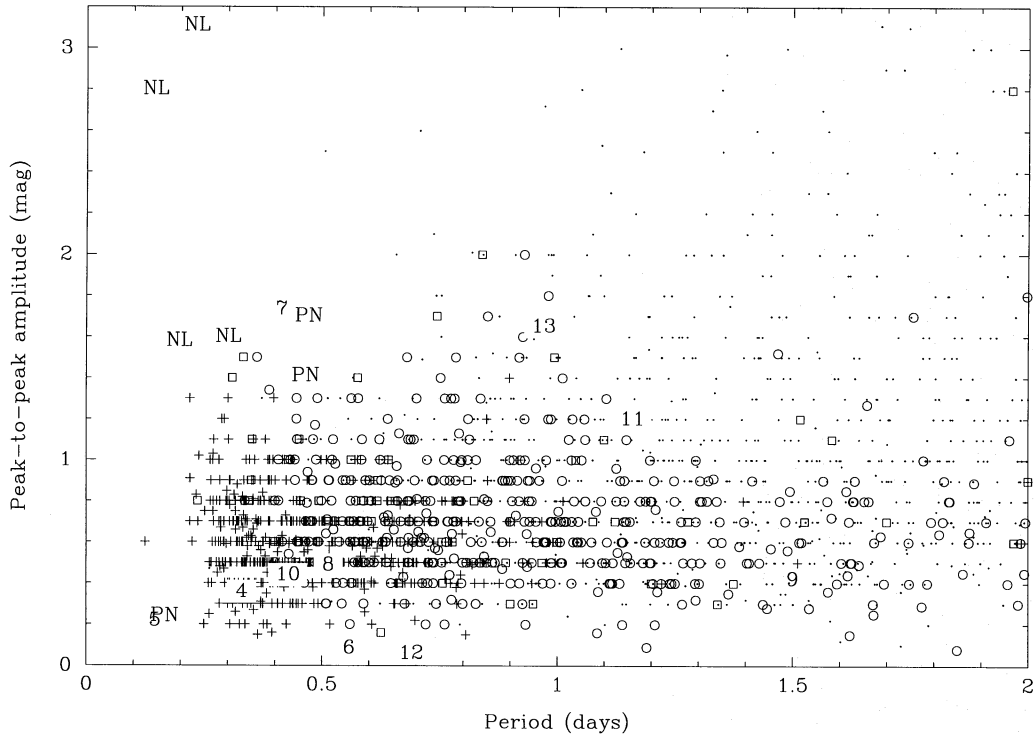

FIG. 11.—Plot of period vs. amplitude (peak-to-peak in magnitude) for eclipsing binaries from the GCVS (Khopolov et al. 1985). Symbols represent, using the nomenclature from the GCVS: *open square* ≡ E, *filled circle* ≡ EA, *open circle* ≡ EB, + ≡EW, NL ≡ EA and nova-like, and PN ≡ EA with a planetary nebula. Variables 4–13 are also plotted.

Lyrae variable. However, the shape of the light curve shown in Figure 9 appears to discount this possibility because of the difference in depth between the primary and secondary minima. Based on this comparison with other types of variable stars, we suggest that variable 7 may be a type of CV.

The variable 5 also occupies an unusual position in Figure 11 if we assume that the peak in the power spectrum gives the period. A period of 3.5 hr is shorter than the lower limit of the envelope of EW eclipsing binaries at a period of around 5 hr. We comment that the EW system with a period of 3 hr is probably erroneous, since it has a period that is significantly lower than the other EW variables (it is also labeled in the GCVS with a code describing it as having an uncertain identification).

An Algol containing the nucleus of a planetary nebula has a period and amplitude very close to variable 5 in Figure 11 (the primary star has spectral type G2IB), and the only other eclipsing binary systems with periods shorter than variable 5 are two Algol-type systems containing white dwarfs with much larger amplitudes. A search in the GCVS for other types of variables with periods and amplitudes near that of variable 5 uncovered nine variables, all of them pulsating variables (six δ-Scuti variables, one SX Phe variable and two β Cephei variables), none of which are expected in the region of the CMD, where variable 5 lies.

Since the evidence presented in § 3.3 suggests that variable 5 is unlikely to be an W UMa system and its positions in the CMDs imply that it does not correspond to any known pulsating star, we speculate that it may also be a variety of CV.

3.5. *Search for Cataclysmic Variables*

To examine the possibility of low signal-to-noise variables existing in our data set, a second variable search was made, mainly directed at finding either quiescent dwarf novae or magnetic CVs with emission varying by orbital modulation. Quiescent field dwarf novae typically have $M_B = 7.5$ and $U-B = -0.9$ (Warner 1976), implying that quiescent dwarf novae in 47 Tuc should have $U \sim 20$ (the true range in magnitude is bound to extend fainter than this because of selection effects). Since virtually all CVs have orbital periods between 80 minutes and 12 hr and amplitudes ranging from a few tenths of a magnitude to more than 1 magnitude (Shara et al. 1995), Figure 3 implies that orbital modulation of dwarf novae may be detectable in the 47 Tuc data set.

There are two known types of magnetic CVs, AM Herculis (polar) systems and DQ Her (intermediate polar) systems. The former are probably too faint to be detected in 47 Tuc, since the average absolute magnitude of the Am Her systems in the survey by Cropper (1990) is 10.2 and shifting them to 47 Tuc would give $V = 23.6$, much fainter than our limiting magnitude of $V \sim 20.0$. DQ Her systems are brighter, with an average $V = 20.4$ if shifted to 47 Tuc. Thus, depending on their numbers, these may be detectable in the 47 Tuc data.

This additional variable search used a modification of the search technique outlined in § 2.4.1. The upper limit on the FAP in the search was raised and special attention was given to eliminating time series affected by the *HST* orbital motion. Stars having peaks within 4 minutes of the *HST* orbital period and with an FAP less than 0.2 were eliminated from further analysis, and similar filtering was applied at 2 and 4 times the orbital period. Stars with peaks at periods longer than 11 hr were also discarded.

A careful comparison was then made between the numbers of power spectra having peaks with small FAPs, and the numbers found using Gaussian noise simulations. A

small excess of power spectrum peaks with FAPs less than 5×10^{-4} was found, but this result is marginal and deeper observations of 47 Tuc with WFPC2 would easily test the reality of these candidate variables.

3.6. *Comparison with X-Ray Sources*

Since variables 5 and 7 are CV candidates, a comparison was made between the variable stars discovered in 47 Tuc and the X-ray sources discovered by Verbunt et al. (1993) and Hasinger et al. (1994) using the High Resolution Imager (HRI) of *ROSAT*. The *ROSAT* observations were split into two parts: the first in 1992 April and May, with an exposure time of 3902 s, and the second in 1993 April, with an exposure time of 13,227 s. In the 1992 observation, four sources were found in the core of 47 Tuc (i.e., within one core radius of the cluster center). Two of these sources were detected in the 1993 observations, at identical luminosities within the uncertainty, and one additional source not found in the earlier observations was detected in the core. Using the numbering system given in Table 1 of Hasinger et al. (1994) and adding an "X" prefix to avoid confusion with the F336W variable stars, sources X8 and X10 must have faded by factors of ~ 6 and ~ 4, respectively, between the observations of 1992 and 1993, and source X9 must have brightened by a factor of ~ 7.

The statistical uncertainty in the positions quoted by Hasinger et al. (1994) varies between 0".2 and 3".4, depending on the number of counts detected. There are also possible systematic offsets of up to 5" in the X-ray positions—such offsets were found by comparing the positions of X-ray sources with the positions of known optical counterparts in other HRI observations. Hasinger et al. (1994) discuss two stars close to their X-ray positions, CPD-72 35B, which is 0".2 from source X6 (positional uncertainty, $\sigma = 1".6$) and HD 2072, 4" from source X12 ($\sigma = 1".3$). The magnitudes of these two stars are $V \simeq 11.7$ and $V \simeq 9.8$, respectively. Hasinger et al. (1994) point out that CPD-72 35B is close to the bright end of the asymptotic giant branch in 47 Tuc, as found by Hesser et al. (1987), Aurière & Ortolani (1988), and in our *HST* observations. It would be surprising if a giant star in 47 Tuc had a relatively high X-ray luminosity (Hasinger et al. 1994), which would be evidence against the identification of CPD-72 35B with X-ray source X6. Furthermore, the chance of finding a positional coincidence only 52".8 from the core of 47 Tuc is relatively good, since the stellar densities there are very high.

A correct positional match for HD 2072 with source X12 appears more likely. HD 2072 is 361" ($15.7 r_c$) from the core of 47 Tuc and is located on the opposite side of 47 Tuc from the SMC. Also, HD 2072 is too bright to be a member of 47 Tuc, and its visual magnitude and reddening imply a distance of ~ 100 pc, at which the observed count rate corresponds to $L_X \simeq 6.6 \times 10^{28}$ ergs s^{-1}, within the expected range for a late type main-sequence star (Hasinger et al. 1994). Henceforth, we assume identification of X12 with HD 2072.

To search for positional coincidences between the X-ray sources and our variable stars, we plot in Figure 12 the positions of all of the stars near the core of 47 Tuc, with labels for the variables and X-ray sources. The positions of Hasinger et al. (1994) have been corrected for precession and the $\sim 4"$ offset of X12 from HD 2072. We have also plotted the relatively large error circles for sources X8 and X10—the error circles for sources X5, X7, and X9 are only

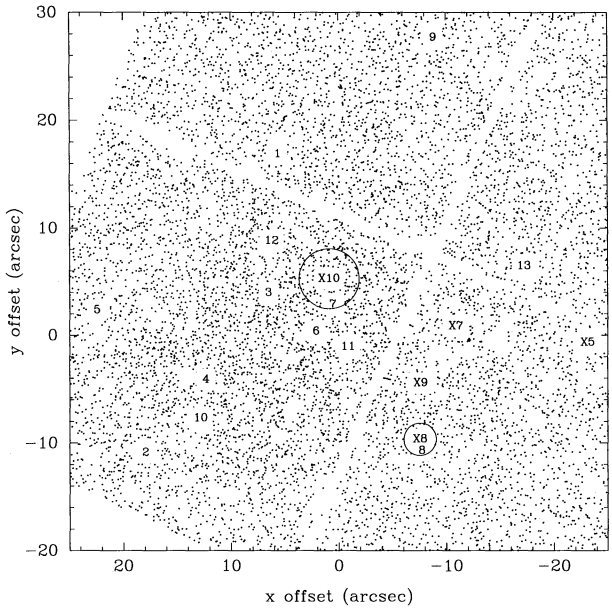

FIG. 12.—Positions of stars near the core of 47 Tuc, relative to star "E" in Guhathakurta et al. (1992). Numeric symbols mark the 47 Tuc variables and the X-ray sources from Hasinger et al. (1994). Error circles for X10 and X8 are also shown.

0".5, 0".2, and 0".2, respectively. Sources X10 and X8 both contain variable stars inside their error circles, suggesting that the X-ray sources are directly associated with the variable stars. This possibility is strengthened if we consider two other factors.

First, the position angles and distances of variables 7 and 8 with respect to the sources X8 and X10 are very similar, in such a way that a further offset in the positions of the X-ray sources of just over 1" would cause source X8 and variable 8 to coincide to $\lesssim 0".3$, and source X10 and variable 8 to coincide to $\lesssim 1".0$, both of which are well within the uncertainties for the two X-ray sources. This $\sim 1"$ offset would not be unusual, seeing that (1) there is a 1".3 uncertainty in the position of source X12, which was used to calculate the offset between the *HST* and *ROSAT* positions, and (2) source X12 is some distance from the core of 47 Tuc, so a slight tilt in the coordinate axes may not be unexpected.

The second and more important factor is the special character of variables 7 and 8. These two variables are comfortably the faintest of the 13 variable stars found in 47 Tuc, with U magnitudes of 19.9 and 19.1. Besides variable 5, with $U = 18.7$, no variable star has a U magnitude fainter than 17.9. The eclipsing binary systems 7 and 8 may therefore represent a different class of star than the eclipsing binaries found near the main-sequence turnoff both in 47 Tuc and in M71 (Yan & Mateo 1994). It also means that they are more likely to contain dark stellar remnants, such as neutron stars or white dwarfs (similar objects were not found in M71, not surprisingly, since few X-ray binaries are expected in this less dense GC). Also, as pointed out earlier, X-ray sources X8 and X10 are both variable, possibly indicating accretion onto a compact source.

Hasinger et al. (1994) claim that the five X-ray sources discovered in the core of 47 Tuc are unlikely to be CVs because they all have $L_X(0.5\text{–}2.5 \text{ keV}) \gtrsim 5 \times 10^{32}$ ergs s^{-1}. This is about an order of magnitude greater than the highest X-ray luminosity observed in the *ROSAT* All Sky

Survey for CVs with known distance and for which a reliable luminosity can be calculated. Hasinger et al. (1994) argue, instead, that the core sources may be binaries in which a neutron star accretes matter at a low rate. Soft X-ray transients (SXTs) have X-ray luminosities consistent with those of the 47 Tuc sources. This differs from the CV interpretation given by Grindlay et al. (1995) for the X-ray sources in NGC 6397.

Indeed, evidence exists that the population of X-ray sources in 47 Tuc is different from that found in two other dense GCs, NGC 6397 and NGC 6752. Grindlay (1995) estimates that there may be as many as 30 sources within the central 80″ of 47 Tuc with luminosities $\gtrsim 10^{32}$ ergs s^{-1}, compared with the roughly five sources with luminosities of 2.2–8.5 $\times 10^{31}$ ergs s^{-1} found in NGC 6397 (Cool et al. 1993). Also, many of the bright sources in 47 Tuc show significant variability in their X-ray luminosity (factors of at least ~ 6, ~ 4, and ~ 7 were found for three of the sources, as listed above), whereas there are smaller limits ($\lesssim 2$) on the variability of the sources in NGC 6397 (Grindlay 1995). Although the luminosities of X8 and X10 are consistent with that of DQ Her systems, an argument against this interpretation is that such systems do not have significant X-ray variability (Patterson 1994).

The three X-ray sources discovered in NGC 6752 have luminosities of 1.1–2.0 $\times 10^{32}$ ergs s^{-1} (Grindlay 1995), brighter than the sources in NGC 6397 but still fainter than most of the 47 Tuc sources (note that the distances to 47 Tuc and NGC 6752, 4.6 kpc and 4.1 kpc, respectively, are comparable, but 47 Tuc is 4 times as luminous as NGC 6752). While strong variability has been found in the nine sources detected in 47 Tuc, no significant variability has been detected in the NGC 6752 sources (Grindlay 1995). A further hint that the population of X-ray sources in 47 Tuc differs from those in NGC 6397 and NGC 6752 is that 47 Tuc contains comparable numbers of X-ray sources ($\gtrsim 9$) and millisecond pulsars ($\gtrsim 11$), as pointed out by Grindlay (1995), yet no millisecond pulsars have been reported in either NGC 6397 or NGC 6752. NGC 6397, at least, has been observed several times by Manchester (see Grindlay 1995).

These differences suggest that the stronger X-ray sources found in the core of 47 Tuc, including, by association, variables 7 and 8, are different from those found in NGC 6397 and NGC 6752. They could be either SXTs (as argued by Hasinger et al. 1994), magnetic CVs, or they may represent a new class of X-ray binaries. Spectroscopic study with HST has the potential to distinguish between SXTs, magnetic CVs, and dwarf novae.

In addition to the point sources, Hasinger et al. (1994) find extended X-ray emission from the core, extending to about $2.6r_c$ from the center. They argue that this emission may be the cumulative emission from a number of low-luminosity sources, possibly CVs, as well as more neutron star binaries.

3.7. *W UMa Simulations*

To estimate the frequency of contact binary systems in 47 Tuc, simulations have been run to test the sensitivity of our results to detecting W UMa stars. To summarize our procedure, we first added simulated stars with a broad range of magnitudes to the average PC images. Then, we repeated our use of DAOFIND in order to estimate the fraction of these stars that would be labeled as stellar. Independently, we calculated light curves for a sample of simulated W UMa stars and applied power spectrum analysis to determine what percentage of these stars were detectable based on the time series alone. These two calculations were combined to determine what percentage of W UMa stars in our 47 Tuc field should be detectable using our reduction techniques.

For the DAOFIND simulations, 1500 stars with magnitudes ranging from $U = 15$ to $U = 23$ were added to the average oversampled images for each CCD. The positions of the stars were randomly chosen with the exception of two constraints: (1) stars were not added within 4 pixels of the edge of the CCD or pyramid shadow, and (2) stars were not added within 9 pixels of the position of any other simulated star. The first constraint removes the influence of edge effects and is acceptable since we remove stars within 4 pixels of edges in our analysis. The second constraint ensures that the simulated stars are a significant distance apart, in such a way that the statistics of the image are not changed by their inclusion.

The PSF used for the simulations was a Lorentz function with the following form: $f(x, y) = A/(1 + z^2)$, where $z^2 = x^2 + y^2$. From $z = 5$ to $z = 10$ pixels, the Lorentz function was multiplied by a function that varied linearly from 1 to 0 in order to truncate the function at large radii. This function is a reasonably crude approximation to the PSF of the *HST* PC, but a more detailed treatment of the PSF is unnecessary for these simulations since (1) the flux in the PSF is dominated by the core, in which the measured PSF is modeled fairly accurately (particularly at the faint limit of the simulations, where incompleteness starts to become a problem), and (2) the incompleteness in our search for W UMa systems will be shown to be dominated by noise levels in the intensity time series, rather than in the star detection procedure. This is expected because of the high signal-to-noise ratio in the average image compared to the ratio in the individual images. Another potentially important factor is our constraint that the average intensity be positive—we did not attempt to model whether this had a significant effect on the detection levels, but the relatively high noise levels in stars with clearly positive intensity (such as variable 7) shows, again, that the noise in the intensity time series dominates the completeness levels.

The criteria used for detection of a simulated star with DAOFIND was that a star be detected within 1 pixel of the input position of the simulated star. Figure 13 shows the detected fraction of stars as a function of magnitude (*dotted line*), with incompleteness setting in at $U \approx 21$.

The distribution of W UMa stars used in these simulations was derived from the data published by Mochnacki (1985) and Rucinski (1994). A Gaussian distribution was fitted to the $B-V$ colors provided by Mochnacki (1985), and linear relationships were determined between the $B-V$ colors and the following W UMa properties: (1) the mass ratio, q, using the data from Mochnacki (1985), (2) the absolute magnitude, using Rucinski (1994), and (3) the orbital period, also using Rucinski (1994).

Using the measured distance modulus to 47 Tuc (Hesser et al. 1987) and our average value of $U-V$ as a function of V, the absolute magnitudes determined above were converted into U magnitudes. The resulting magnitude distribution extends from ~ 15.5 mag to ~ 21.5 mag, with a peak at around 18.5 mag (Fig. 13, *dot-dashed line*).

To determine the light curves for the W UMa simulations, the light curves presented by Rucinski (1993) were

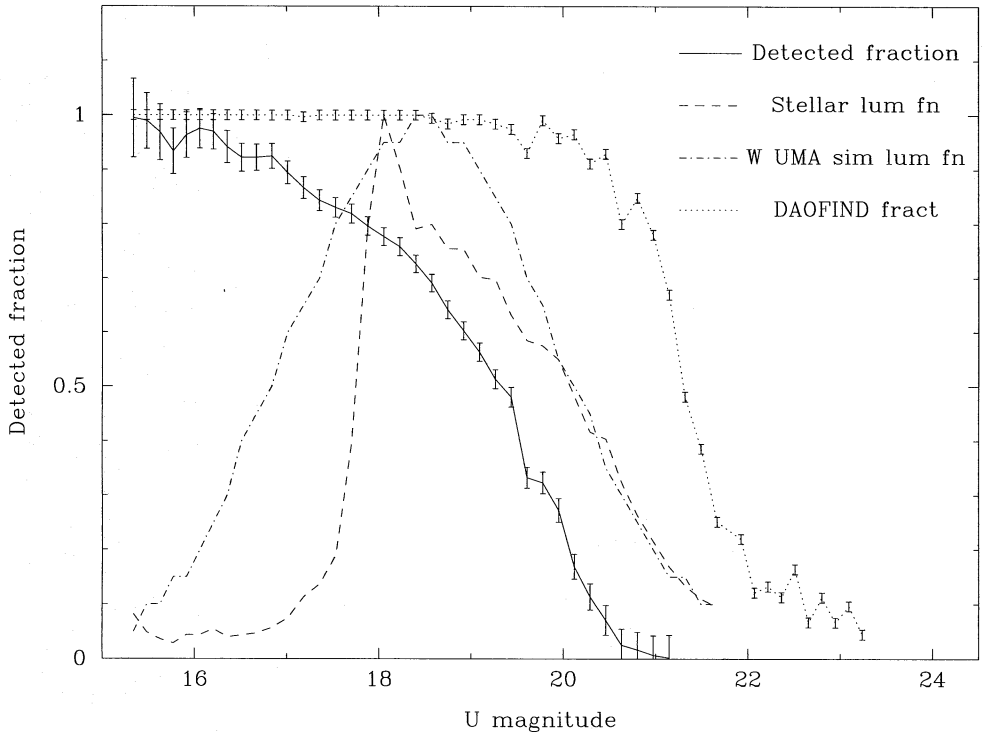

FIG. 13.—A plot summarizing the results of the W UMa simulations; detectability as a function of U

again used. We assumed that $f = 0$, guided by previous estimates of this parameter for W UMa systems (Rucinski 1993). For each magnitude step used in the simulations, a set of orbital inclinations evenly spaced between 0° and 90° was used. The number of simulations generated at each angle was then weighted by sin (i), in order to allow for selection effects along our line of sight. When these assumptions are combined with the previously calculated distributions of q and the orbital period (assuming random initial orbital phases), the light curves for the W UMa stars are completely specified, apart from the noise component. This component was estimated from the real stellar time series for 47 Tuc, using both the measured variation of the time series rms as a function of magnitude, and the Gaussian distribution of the time series (using the Kolmogorov-Smirnov test, Press et al. 1992, we were unable to reject the hypothesis that the measured distribution was consistent with a Gaussian distribution). Using the measured noise values means that we account, realistically, for additional uncertainties introduced by near neighbor effects, flat field uncertainties, CCD defects, and residual low-energy cosmic rays.

The time series were converted into power spectra, as done with the analysis of the measured data. A variable star was considered to be detected if the FAP probability of the peak at the injected orbital period (or twice the orbital period) was less than 1×10^{-4}. The resultant fraction of W UMa systems detectable in our data set was then obtained by multiplying the fraction of stars found using DAOFIND by the fraction of W UMas found in the power spectra analysis. Figure 13 shows as functions of U magnitude the total fraction of W UMas detectable, along with the fraction of stars detected using DAOFIND alone. Also plotted is the stellar luminosity function for 47 Tuc from this data set (normalized to one, and not corrected for incompleteness), and the luminosity function for the W UMa simulations. Figure 14 shows the average detection efficiency for the simulations as a function of distance from the center of 47 Tuc, and it shows a small but significant increase in detection efficiency with distance. This effect is caused, in part, by PC8, which has a higher sensitivity to oscillations and is the only source of stars at distances greater than ~47″ from the cluster core.

The contact binary frequency for the core of 47 Tuc can now be estimated. Two W UMa variables have been found in our data set (variables 4 and 6). To estimate the number of stars sampled in our variable search, we choose a magni-

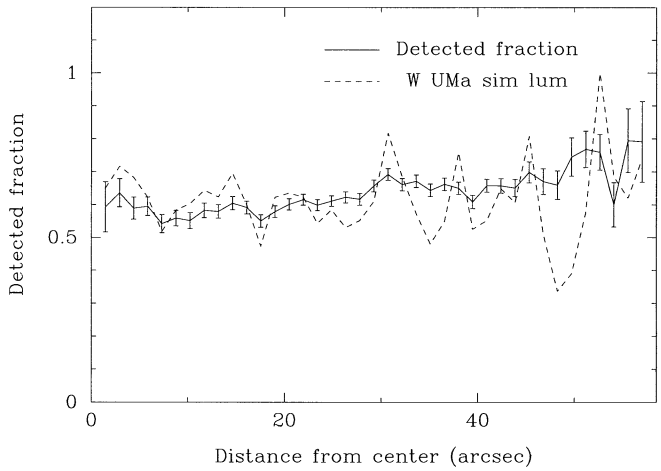

FIG. 14.—Further W UMa simulation results; detectability as a function of distance from the cluster core.

tude cutoff of $U = 19.0$ so as to ensure a high level of completeness (the above simulations then imply a total detection efficiency of 77%). This also minimizes the number of spurious stellar detections and ensures negligible contamination in our sample from bright stars in the SMC. Correcting for completeness, we have detected 2.6 W UMas in the 7700 stars that are brighter than our cutoff, for a contact binary frequency of 0.03%. Since most other workers quote the contact binary frequency among main-sequence stars, we have detected 1.3 W UMas in 6135 main-sequence stars (removing the stars brighter than the main-sequence turnoff), for a contact binary frequency of 0.02%.

4. DISCUSSION

4.1. *Binary Radial Distribution*

Previous work on the radial distribution of binaries has been hampered by the small number of binaries detected in GCs and the difficulties in doing photometry near the cores of clusters. Pryor et al. (1989) analyzed the radial distribution of binaries discovered in six clusters. All of these clusters have half-mass relaxation times shorter than their ages, implying that the binaries should be centrally concentrated. Surprisingly, however, the binaries appeared to have the same distribution as the giants and upper main-sequence stars that produce the light in the clusters. Though the sample consisted only of six binaries, the expected distribution for a sample of 1.8 $M_\odot$ binaries could be rejected at the 98% confidence level.

Kaluzny & Krzeminski (1993) detected a relatively large number of binaries (9) in NGC 4372, but do not discuss whether they are more centrally concentrated than the average stellar distribution. Their photometry suffers from a large degree of incompleteness, particularly in the central parts of the cluster. Yan & Mateo (1994) report that the eclipsing binaries they discovered in M71 do not show any significant central concentration. However, their false-star experiments show that increased crowding near the cluster center reduces their sensitivity to variability. Yan & Reid (1996) found six short-period binary systems in M5, but their simulations show severe incompleteness at distances less than $3r_c$–$4r_c$ from the cluster core, which is not surprising for ground-based observations of this moderately high density cluster.

With the increased resolution of the *HST* images, the 47 Tuc data are not seriously hampered by the increased crowding near the cluster core, as shown by Figure 14. The cumulative radial distribution of the binary stars discovered in 47 Tuc is shown in Figure 15. Two different distributions are plotted for the binaries, one for the full list of 10 candidate binaries (variables 4–13) and the other a subset of this list ("confirmed binaries"), by excluding variables 5 and 12. For comparison, we also plot the radial distribution of all of the stars in our cleaned star list with $15.9 < U < 20.4$, the range in average U mag of the confirmed candidates, and the radial distribution of the BSS discovered by Guhathakurta et al. (1996). It appears from Figure 15 that the radial distributions of the binaries and the BSS are similar, and that both are more centrally concentrated than the "normal" stars (Guhathakurta et al. 1992 has already used *HST* to show that the BSS in 47 Tuc are more centrally concentrated than the normal stars). All but one of the 10 binary candidates are found within $1r_c$ of the center (the

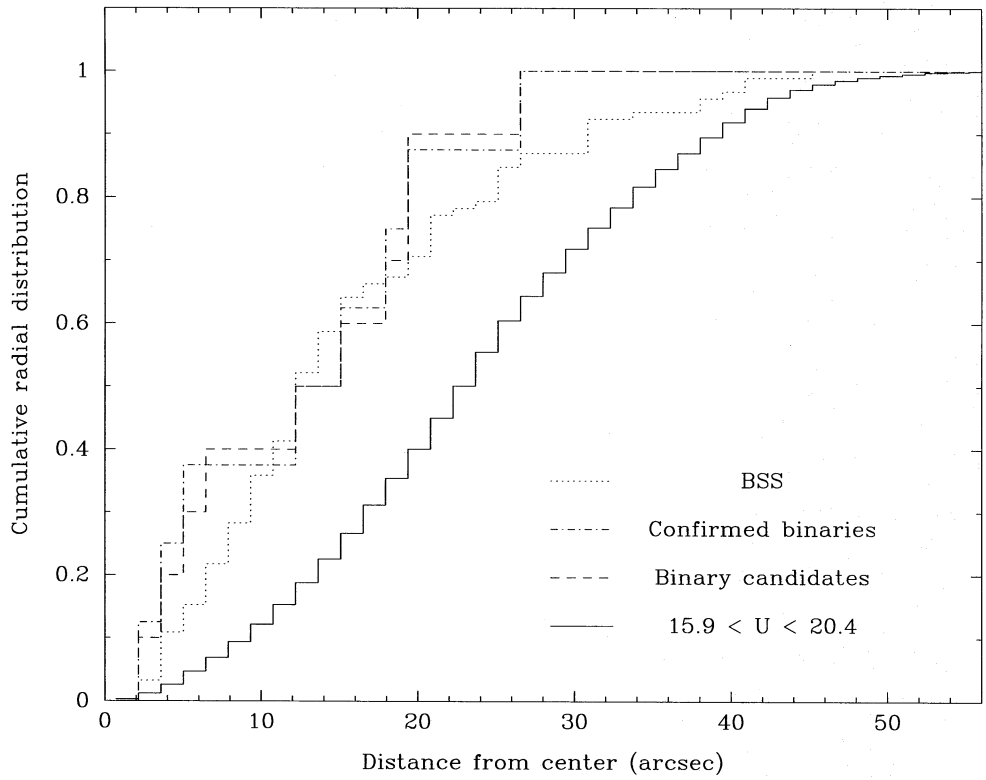

FIG. 15.—Cumulative radial distributions of all main-sequence, subgiant, and giant stars with the same magnitude range ($15.9 < U < 20.4$) as the binary stars detected in 47 Tuc, plotted as an unbroken line. Radial distributions of the binary systems and BSS are also shown.

exception lies at $1.2r_c$), although only 49.8% of all stars with $15.9 < U < 20.4$ are found within one core radius.

Although the sample size of the binaries is small, the Kolmogorov-Smirnov test rejects the null hypothesis that the stars with $15.9 < U < 20.4$ and the 10 binary candidates have the same radial distribution at the 99.2% confidence level (96.7% for the confirmed binaries). The hypothesis that the radial distributions of BSS and binaries are the same can only be rejected at the 20% and 19% confidence levels for the candidate and confirmed binaries, respectively.

This strong central concentration for the binaries in 47 Tuc, as predicted by theory (see Hut et al. 1992), and the similarity between the binary and BSS distributions are even more striking when compared with the work of Kaluzny & Krzeminski (1993) and Yan & Mateo (1994). While incompleteness caused by crowding affects the NGC 4372 data, it is interesting to note that the oscillating SX Phe variables detected by Kaluzny & Krzeminski (1993; all BSS) *are* found to be concentrated toward the core of NGC 4372, which is consistent with the results of Sarajedini (1993), who found the BSS to be centrally concentrated. Using the data of Kaluzny & Krzeminski (1993) for NGC 4372, we are able to reject the hypothesis that the eight oscillating BSS and the nine short-period binaries have the same radial distribution at the 97.1% confidence level.

For the binary distribution in NGC 4372 to resemble that of the oscillating BSS, a large binary sample would have to remain undetected in the core of this cluster. It would be surprising, however, if the oscillating BSS were easier to detect near the cluster core than the contact binaries, since the data of Kaluzny & Krzeminski (1993) shows that they have a smaller average light-curve amplitude (0.36 mag) than the close binaries (0.48 mag), as expected for these stellar types. This difference in amplitude will, at least partially, compensate for the average difference in magnitude between the oscillating BSS and the fainter binaries (0.37 mag). The time sampling should not be an important factor, since the observations of Kaluzny & Krzeminski (1993) last a total of 29.9 hr.

Since the central relaxation time for 47 Tuc of 7.4×10^7 yr (Webbink 1985) is much smaller than that for NGC 4372 (1.3 Gyr), a difference between the binary radial distributions for these two clusters may not be unexpected. However, a clear difference between the BSS and binary distributions in NGC 4372 is somewhat surprising if the merger of primordial binaries is responsible for the formation of the BSS (neglecting the effect of encounters between binaries). Under this hypothesis, the BSS should have formed from the primordial binary population, and the binaries and BSS should have roughly equal masses and have had equal amounts of time to sink to the cluster core.

The radial distribution of the binaries and BSS in M71 also appears unusual when compared to 47 Tuc. Yan & Mateo (1994) find no significant central concentration for the binaries in this cluster (all five of the eclipsing binaries are found more than $1.6r_c$ from the center, two of them more than $4.5r_c$, and only one of the five stars, a distance $2.0r_c$ from the center, is considered likely to be a foreground object). This lack of central concentration for the binaries in M71 contrasts with the very centrally concentrated BSS distribution found by Richer & Fahlman (1988). For the distribution of binary stars to resemble that of the BSS, again a large sample of eclipsing binaries would need to be found in the core. Although crowding is a problem for detecting variable stars near the cluster core (Yan & Mateo do not give details of their completeness analysis), it may be surprising if binaries with the same properties as those found in the outer regions of the cluster would not be detected nearer the core, since Yan & Mateo (1994) estimate that the detected binaries are all over 2 mag brighter than their average limiting magnitude for finding binaries, and M71 qualifies as a low-density cluster.

These results imply that the binaries in 47 Tuc are probably more centrally concentrated compared to other cluster stars than the binaries in M71 and NGC 4372. Because the observations of M71 only sample from $\sim 0.1r_t$ to $\sim 0.3r_t$ (where r_t is the tidal radius), it is still possible that the binaries in this cluster are more centrally concentrated than the average cluster star, as pointed out by Yan & Mateo (1994), even without finding large numbers of binaries closer to the core.

The effect of mass segregation on these distributions is difficult to estimate because 47 Tuc is much more centrally concentrated [$\log (r_t)/\log (r_c) = 2.08$; Webbink 1985] than M71 or NGC 4372 [$\log (r_t)/\log (r_c) = 1.13$ and 1.09, respectively; Webbink 1985]. As pointed out by the referee, Tad Pryor, differences in central concentration change the appearance of the mass segregation, in such a way that detailed modeling is required to understand the significance of the different radial distributions.

If the radial distribution of binaries in 47 Tuc is more centrally concentrated than in NGC 4372 or M71, this suggests a possible difference in the binary formation mechanism between the high and low-density clusters. The simplest interpretation is that, while the binaries found in NGC 4372 and M71 are believed to be primordial, short-period binaries have been formed in the core of 47 Tuc, e.g., from the interactions of wide binaries. This possibility will be considered further below and in Edmonds & Gilliland (1996b). The reasons for possible differences between the binary and BSS radial distributions in 47 Tuc and the two low-density clusters are not immediately obvious, and they warrant further observations to increase the statistics and radial extent of the binary samples. A possible explanation will be presented in Edmonds & Gilliland (1996b).

4.2. *Contact and Detached Binaries*

The most popular scenario for the formation of W UMa systems is that initially detached binary systems experience orbital angular momentum loss (AML), via magnetic torques from a stellar wind, in a situation in which the spin angular momentum and the orbital angular momentum are tidally coupled (Huang 1967; Vilhu 1982; Guinan & Bradstreet 1988). The models suggest that binaries with initial orbital periods of 2.5–5 days should evolve into contact systems after 3–14 Gyr. Once the contact system has been formed, simple arguments show that such binaries *must* eventually merge into a single star (Webbink 1976; Rahunen 1981; Guinan & Bradstreet 1988). The timescale for this process ($\tau_{\rm merge}$) is extremely uncertain, with estimates ranging between 0.1 and 10 Gyr (van't Veer 1979; Rahunen 1981; Eggen & Iben 1989). Most studies seem to favor ~ 1 Gyr.

Observational evidence suggests that primordial binaries probably do not have periods $\lesssim 2.5$ days, since this value is the shortest period observed in zero-age binary populations studied by Giuricin, Mardirossian, & Mezzetti (1984), Mathieu, Walter, & Myers (1989), and Bodenheimer, Ruz-

maikina, & Mathieu (1993). If there is a lower limit to the primordial binary period, then the AML theory implies that the youngest open clusters should contain no W UMa systems. The age for this expected cutoff is about 3–5 Gyr. Indeed, Kaluzny & Shara (1988) did not find a single W UMa type system in a survey of clusters with ages less than 4 Gyr. However, Kubiak et al. (1992) have discovered 6 W UMa systems in Tombaugh 2, a cluster with an age of only $\sim$2 Gyr. Rather than the failure of the AML scenario, this observation may indicate either that AML is more efficient and rapid than previously thought, or that the 2.5 day lower limit on the period of primordial binaries is too high.

Another factor affecting the rate of formation of close or contact binaries is the possibility that binaries can come into contact (forming W UMa systems) or undergo mass transfer (forming Algol systems) as a direct result of the evolutionary expansion of the primary star (Yan & Mateo 1994). The radii of primaries near the main-sequence turnoff is $\sim$90% larger than when they were on the main sequence (Vandenberg & Bell 1985). Yan & Mateo (1994) argue that this expansion might explain the clustering of eclipsing binaries near the turnoff (the "crowding effect") in M71. Furthermore, they argue that if evolutionary expansion is the correct explanation of the crowding effect, then some or all of the short-period binaries in M71 may have evolved into contact systems more rapidly than predicted by the AML theory. This complication is important for 47 Tuc, since a similar clustering of main-sequence binaries near the turnoff is also seen for this cluster, particularly if variables 5, 7, and 8 are all CVs.

Another prediction of the AML theory is that W UMa systems should have had time to form in older open clusters, and, indeed, rich populations of contact binaries have been found in these clusters. For example, Kaluzny & Shara (1987) found at least seven W UMa systems in NGC 188 (with periods from 0.286 to 0.586 days) and three longer period variables (with periods of >1.6 days, >0.8 days, and 1.3 days). This cluster has an age of 6–10 Gyr (Maceroni & van't Veer 1991). Kaluzny et al. (1993) found 11 contact binaries with periods ranging from 0.225 days to 0.546 days and one eclipsing binary with a period of $\sim$1 day in Berkeley 39 (a cluster with an age very close to that of NGC 188; Kaluzny et al. 1993), and Kaluzny & Rucinski (1993) discovered eight contact binaries, all with periods less than 0.4 days, and four Algol type systems with periods $\gtrsim$1 day in NGC 6791 (age $\sim$6.5–10 Gyr; Kaluzny & Rucinski 1993). Finally, Gilliland et al. (1991) found three W UMas with periods of 0.44 days, 0.36 days, and 0.27 days among the brightest 130 stars in a small area of M67 (with an age of $\sim$4–5 Gyr).

The observationally more difficult discoveries of the longer period Algol systems are important because they provide obvious progenitors for the next generation of contact binaries—the absence of these in earlier observations had been noted as a problem for the AML scenario for the formation of W UMa systems (Leonard & Linnell 1992). While the relative incidence of W UMa systems among F–K disk dwarfs is estimated at 0.1%, the relative frequency for the clusters listed above is more than an order of magnitude higher.

For the older GCs, the long-period limit in the AML theory becomes significant. Above a period of $\sim$5 days, binaries are no longer believed to be affected by AML because, beyond a certain stellar separation, tidal coupling and AML are ineffective in producing orbital shrinkage (Eggen & Iben 1989).

Since GCs are usually at least twice as old as open clusters, the AML theory for contact binaries would predict that GCs contain a smaller frequency of contact binaries than the older open clusters, since some of the shorter period contact binaries will already have merged into single stars (we assume here that there are no dynamical complications producing or destroying binaries such as binary-binary collisions or tidal captures—see Edmonds & Gilliland 1996b). A small number of short-period Algol systems may also be observable, but no eclipsing binaries with periods longer than $\sim$1–2 days, since all primordial binaries with periods between 2.5 and 5 days should have had time to evolve into close binary systems with periods much shorter than a day.

Eclipsing binary systems have been found in several GCs (all with lower stellar density than 47 Tuc). Niss, Jorgensen, & Lautsen (1978) found an Algol system in Ω Cen with a period of 1.38 days, Mateo et al. (1990) found two W UMa systems in NGC 5466 with periods of 0.342 and 0.298 days and an Algol with a period of 0.511 days, and Irwin & Trimble (1984) found two W UMa systems in M55 with periods of 0.254 and 0.245 days. The Mateo et al. (1990) observations were capable of detecting binaries with periods as long as $\sim$2–3 days. One W UMa system with a period of $\sim$0.3 days was discovered in NGC 6496 (Hut et al. 1992). Kaluzny & Krzeminski (1993) discovered eight W UMa systems in NGC 4372, all with periods less than 0.41 days, and one Algol with a period of 0.4 or 0.8 days. Two other variables of unknown type were found with periods of 3.31 and 2.6 days (or twice these), both possibly binaries. Yan & Mateo (1994) discovered two W UMa systems in M71 with periods between 0.35 and 0.41 days and an Algol system with a period of 0.56 days. Their upper limit on detection of variables was around 5 days. Yan & Reid (1996) discovered five W UMa systems in M5 with periods between 0.41 days and 0.70 days and one Algol with a period of 0.63 days. Their observations were of 11.4 hr duration. Finally, Mateo & Mirabel (1995) found 3 W UMa systems in M55. After correcting for incompleteness, the relative frequencies of the W UMa detections compared to main-sequence stars (where available), are 0.09% (NGC 6496), 0.03% (M55), 0.25% (M5), and 0.14% (M71), compared to 0.02% for 47 Tuc.

These results are mostly consistent with the predictions outlined above. The relative frequencies of W UMa systems in GCs are all smaller than those in open clusters and there are relatively few instances of long period binary systems, although searches for the latter are in some cases incomplete. The exceptions merit special attention. The 1.38 day Algol system may be the result of binary-binary collisions and thus may be much younger than the age of the cluster—Ω Cen has a higher density than most of the clusters discussed above, increasing the chances of these collisions. The two possible long period binaries in NGC 4372 may both be primordial binaries with periods long enough to make AML relatively inefficient.

The population of binaries detected in 47 Tuc appears to be fundamentally different from populations discovered in other globular and open clusters. First the frequency of W UMa systems among main-sequence stars in 47 Tuc is lower than that found in other GCs. Second, and perhaps more significantly, there are 3 binary systems in 47 Tuc with

periods around a day or longer, and 6 eclipsing binaries with β-Lyrae or Algol-type light curves, compared to only 2 W UMa systems. These results, particularly the detection of the longer period binaries, suggest that, if the AML theory for close binaries is correct, at least some of the binary systems detected in 47 Tuc are not primordial short-period binaries, but have been formed in the cluster core. The AML theory predicts that all primordial binaries with periods $\lesssim 5$ days would have had sufficient time to evolve into shorter period binaries. Note that recent observations of the core of the dense GC NGC 6752 by Rubenstein & Bailyn (1996) have discovered evidence for binaries, but with no detection of W UMa systems. Their observations were of about 20 hr duration and so they may have missed longer period systems. These observations provide further evidence for binary production in the cores of dense GCs.

5. CONCLUSION

5.1. *Summary of Results*

We have shown that the W UMa frequency among main-sequence stars in 47 Tuc is lower than that for lower density GCs. Furthermore, the presence of three binaries with periods of around a day or longer and several other semi-detached binaries suggests that, if the AML scenario is correct, at least some of the binaries are not primordial. The radial distribution of the binaries is strongly centrally concentrated and is similar to that of the BSS, implying a strong link between the formation mechanisms of the binaries and the BSS (indeed, one of the BSS is a W UMa system and a detached binary may also be a BSS).

The possibility that the centrally concentrated binaries were formed in the core of 47 Tuc is consistent with the hypothesis given by Bolte, Hesser, & Stetson (1993) that the primordial binaries in the core of dense GCs have mostly been destroyed but that binary formation and collision mechanisms may be important, producing the centrally concentrated populations of BSS in the dense cores of clusters like 47 Tuc and NGC 6397. These conclusions are similar to those of Bailyn (1992) and Ferraro, Fusi Peci, & Bellazzini (1994). A detailed treatment of single and binary star interactions in 47 Tuc has been carried out by Davies & Benz (1995), but a comparison is beyond the scope of this paper (see Edmonds & Gilliland 1996b).

Recently, *HST* has been used to search for binaries in the core of another dense GC, NGC 6752. Shara et al. (1995) used the Faint Object Camera to monitor 730 stars in the core of NGC 6752. The 31 FOC images spanned a time of 7 hr and were deliberately offset slightly from the core, in such a way that they covered about 40% of the inner core radius and 25% of the volume between r_c and $2r_c$. The complete lack of variables found is difficult to understand, given the sampling of stars near the core and the sensitivity to stars well down the main sequence. At first glance, this result appears to be inconsistent with our results for 47 Tuc. However, the number of stars searched for variability in this cluster is almost a factor of 20 smaller than the number searched in 47 Tuc. Furthermore, since NGC 6752 is a dense cluster, with $\log(\rho_0) = 4.48$ (Webbink 1985), most of the binaries should reside within $1r_c$ of the cluster core, and the survey by Shara et al. (1995) missed some 60% of the inner core radius. Also, the core density is ~ 3.5 times lower in NGC 6752 than for 47 Tuc, therefore, tidal captures and stellar collisions would not have been as high. Finally, several of the longer period binaries found in 47 Tuc would probably have been missed with the much shorter NGC 6752 observations. We conclude that a lack of binaries in the survey by Shara et al. (1995) is probably not inconsistent with the detection of binaries in 47 Tuc, particularly in view of the Rubenstein & Bailyn (1996) detection of binaries in the core of this cluster using the larger field of the PC with WFPC2 and a longer observing time of ~ 20 hr.

5.2. *CVs and Neutron Star Binaries*

While the frequency and period distribution of the binaries discovered in 47 Tuc seem consistent with binary formation taking place in the cores of dense clusters, the general paucity of CVs in 47 Tuc and other dense GCs is a recognized problem, particularly when compared with the predictions of tidal capture theory (see, e.g., Shara et al. 1995; Shara et al. 1996). There are hints, however, that a large population of magnetic CVs or nova-like variables may be present in 47 Tuc, which may explain the dearth of dwarf novae. The possible CVs discovered by Paresce et al. (1992) and Shara et al. (1996) are two candidates. In addition, while the search performed in this paper for CVs via orbital modulation is far from complete, three new candidates for CVs have been found (variables 5, 7, and 8). Since these objects are near the limit of detectability for our data set, they may represent the "tip of the iceberg" for a large population of faint (possibly magnetic) CVs in 47 Tuc.

The probable X-ray sources variables 7 and 8 may also be neutron star binaries rather than magnetic CVs. Since many of the 47 Tuc X-ray sources are highly variable, other sources may easily have been missed, plus the extended emission near the 47 Tuc core probably indicates many lower intensity sources. If neutron star binaries are more common than CVs in GCs, then the ramifications would be significant—for example, it would disagree with the predictions of Davies & Benz (1995) and may be important for the formation of millisecond pulsars. It could be possible, for instance, that neutron stars are involved more easily than white dwarfs in tidal captures, or that neutron stars tend to displace the less massive red dwarfs and white dwarfs in CVs rather easily.

5.3. *Future Observations*

Clearly much more observational work must be done to further test and develop theories of binaries in clusters. Searches for binaries and BSS should be made in GCs spanning the full range in central concentration, and these searches should cover broad ranges in stellar intensity and radial coverage.

Now that the giant and upper main-sequence stars have been thoroughly searched for variability in the core of 47 Tuc using WF/PC, there is enormous potential in carrying out a much deeper search using WFPC2. This search would provide a rigorous search for faint, short-period binaries and all known classes of CV in 47 Tuc. A deep search for orbitally modulated emission from CVs would answer many questions regarding the presence of these objects in the cores of dense clusters. The known CVs alone are important targets, and we would be able to stringently test the new candidate CV/neutron star systems for variability. Excellent light curves and color measurements, in particular, would be obtained for variables 7 and 8. If a large population of neutron star binaries or magnetic CVs is

found in 47 Tuc, there would be potentially far-reaching implications for the study of these exotic binary systems and for tidal capture theory.

We thank Tad Pryor, the referee, for his careful reading of the paper and his excellent suggestions for improving the content of the paper. We also acknowledge Mario Livio for kindly reading an early draft of this paper. This work was supported by NASA through grant GO-4664.01-92A from the Space Telescope Science Institute, which is operated by the Association of Universities for Research in Astronomy, Inc., under NASA contract NAS 5-26555.

REFERENCES

Abt, H. A., & Willmarth, D. W. 1987, ApJ, 318, 786
Aurière, M., Lauzeral, C., & Koch Miramond, L. 1994, in Frontiers of Space and Ground-Based Astronomy, ed. W. Wamsteker, M. S. Longair, & Y. Kondo (Dordrecht: Kluwer), 633
Aurière, M., & Ortolani, S. 1988, A&A, 204, 106
Bailyn, C. D. 1992, ApJ, 392, 519
Bodenheimer, P., Ruzmaikina, T., & Mathieu, R. D. 1993, in Protostars and Planets III, ed. E. H. Levy & J. I. Lunine (Tucson: Univ. Arizona Press), 367
Bolte, M., Hesser, J. E., & Stetson, P. B. 1993, ApJ, 408, L89
Carney, B. W. 1983, AJ, 88, 623
Carney, B. W., & Latham, D. W. 1987, AJ, 93, 116
Cool, A. M., Grindlay, J. E., Cohn, H. N., Lugger, P. M., & Slavin, S. D. 1995, ApJ, 439, 695
Cool, A. M., Grindlay, J. E., Krockenberger, M., & Bailyn, C. D. 1995, ApJ, 410, L103
Cropper, M. 1990, Space Sci. Rev., 54, 195
Davies, M. B., & Benz, Z. 1995, MNRAS, 276, 876
De Marchi, G., & Paresce, F. 1995, A&A, 304, 211
Di Stefano, R., & Rappaport, S. 1994, ApJ, 423, 274
Duquennoy, A., & Mayor, M. 1991, A&A, 248, 485
Edmonds, P. D., & Gilliland, R. L. 1996a, ApJ, 464, L157
———. 1996b, in preparation
Eggen, O. J., & Iben, I. 1989, AJ, 97, 431
Fabian, A. C., Pringle, J. E., & Rees, M. J. 1975, MNRAS, 172, 15
Ferraro, F. R., Fusi Peci, F., & Bellazzini, M. 1994, A&A, 294, 80
Gilhland, R. L., et al. 1991, AJ, 101, 541
Gilliland, R. L., Edmonds, P. D., Petro, L. D., Saha, A., & Shara, M. M. 1995, ApJ, 447, 191 (Paper I)
Giuricin, G., Mardirossian, F., & Mezzetti, M. 1984, ApJS, 54, 421
Grindlay, J. E. 1995, in ASP Conf. Ser., Millisecond Pulsars: A Decade of Surprise, ed. A. S. Fruchter, M. Tavani, & D. C. Backer (San Francisco: ASP), 57
Grindlay, J. E., Cool, A. M., Callanan, P. J., Bailyn, C. D., Cohn, H. N., & Lugger, P. M. 1995, ApJ, 455, L47
Guhathakurta, P., Edmonds, P. D., & Gilliland, R. L. 1996, in preparation
Guhathakurta, P., Yanny, B., Schneider, D. P., & Bahcall, J. N. 1992, AJ, 104, 1790
Guinan, E. F., & Bradstreet, D. H. 1988, in Formation and Evolution of Low Mass Stars, ed. A. K. Dupree & M. T. Lago (Dordrecht: Kluwer), 345
Hasinger, G., Johnston, H. M., & Verbunt, F. 1994, A&A, 288, 466
Hesser, J. E., Harris, W. E. Vandenburg, D. A., Allwright, J. W. B., Shott, P., & Stetson, P. B. 1987, PASP, 99, 739
Horne, J. H., & Baliunas, S. L. 1986, ApJ, 302, 757
Huang, S. S. 1967, ApJ, 150, 229
Hut, P. 1993, in ASP Conf. Ser. 53, Blue Stragglers, ed. R. A. Saffer (San Francisco: ASP), 44
Hut, P., et al. 1992, PASP, 104, 981
Irwin, M. J., & Trimble, V. 1984, AJ, 89, 83
Kaluzny, J., & Krzeminski, W. 1993, MNRAS, 264, 785
Kaluzny, J., Kubiak, M., Szymanski, M., Udalski, A., Krzeminski, W., & Mateo, M. 1995, in ASP Conf. Ser., Binaries in Clusters, ed. G. Milone & J.-C. Mermilliod (San Francisco: ASP), in press
Kaluzny, J., Mazur, B., & Krzeminski, W. 1993, MNRAS, 262, 49
Kaluzny, J., & Rucinski, S. M. 1993, MNRAS, 265, 34
Kaluzny, J., & Shara, M. M. 1987, ApJ, 314, 585
———. 1988 AJ, 95, 785
Khopolov, P. N. et al. 1985, General Catalogue of Variable Stars, Fourth Edition (Moscow: Nauka Publishing House)
Kjeldsen, H., & Frandsen, S. 1992, PASP, 104, 413
Kubiak, M., Kaluzny, J., Krzeminski, W., & Mateo, M. 1992, Acta. Astron., 42, 145
Latham, D. W., Mazeh, T., Carney, B. W., McCrosky, R. E., Stefanik, R. P., & Davis, R. J. 1988, AJ, 96, 567
Leonard, P. J. T. 1989, AJ, 98, 217
Leonard, P. J. T., & Linnell, A. P. 1992, AJ, 103, 1928
Livio, M. 1995, in ASP Conf. Ser., Binaries in Clusters, ed. G. Milone & J.-C. Mermilliod (San Francisco: ASP), in press
Maceroni, C., & van't Veer, F. 1991, A&A, 248, 430
Machin, G., Callanan, P. J., Charles, P., & Naylor, T. 1990, in Accretion-Powered Compact Binaries, ed. C. W. Mauche, (Cambridge: Cambridge Univ. Press), 163
Manchester, R. N., Lyne, A. G., Robinson, C., D'Amico, N., Bailes, M., & Lim, J. 1991, Nature, 352, 219
Mateo, M., Harris, H. C., Nemec, J., & Olszewski, E. W. 1990, AJ, 100, 469
Mateo, M., & Mirabel, N. 1995, in ASP Conf. Ser., Binaries in Clusters, ed. G. Milone & J.-C. Mermilliod (San Francisco: ASP), in press
Mathieu, R. D., Walter, F. M., & Myers, P. C. 1989, AJ, 98, 987
Mayor, M., et al. 1984, A&A, 134, 118
Meylan, G., Dubath, P., & Mayor, M. 1991, ApJ, 383, 587
Mocknacki, S. W. 1985, in ASI Ser., Interacting Binaries, ed. P. P. Eggleton & J. E. Pringle (Paris: ASI), 51
Niss, B., Jorgensen, H. E., & Lautsen, S. 1978, A&AS, 32, 387
Paresce, F., et al. 1991, Nature, 352, 297
Paresce, F., & De Marchi, G. 1994, ApJ, 427, L33
Paresce, F., De Marchi, G., & Ferraro, F. 1992, Nature, 360, 46
Patterson, J. 1994, PASP, 106, 209
Press, W. H., & Teukolsky, S. A. 1977, ApJ, 213, 183
———. 1988, Comput. Phys., 2(6), 77
Press, W. H., Teukolsky, S. A., Vetterling, W. T., & Flannery, B. P. 1992, Numerical Recipes in Fortran (Cambridge: Cambridge Univ. Press)
Pryor, C., McClure, R. D., Fletcher, J. M., & Hesser, J. E. 1989, in Dynamics of Dense Stellar Systems, ed. D. Merritt (Cambridge: Cambridge Univ. Press), 175
Rahunen, T. 1981, A&A, 102, 81
Ratnatunga, K. U., & Bahcall, J. N. 1985, ApJS, 59, 63
Richer, H. B., & Fahlman, G. G. 1988, ApJ, 325, 218
Rubenstein, E. P., & Bailyn, C. D. 1996, ApJ, submitted
Rucinski, S. M. 1993, PASP, 105, 1433
———. 1994, PASP, 106, 462
———. 1995, PASP, 107, 648
Sarajedini, A. 1993, in ASP Conf Ser. 53, Blue Stragglers, ed. R. A. Saffer (San Francisco: ASP), 14
Scargle, J. D. 1982, ApJ, 263, 835
Shara, M. M., Bergeron, L. E., Gilliland, R. L., Saha, A., & Petro, L. D. 1996, ApJ, in press
Shara, M. M., & Drissen, L. 1995, ApJ, 448, 203
Shara, M. M., Drissen, L., Bergeron, L. E., & Paresce, F. 1995, AJ, 441, 767
Shara, M. M., Kaluzny, J., Potter, M., & Moffat, A. F. J. 1988, ApJ, 328, 594
Stetson, P. B. 1987, PASP, 99, 191
Stryker, L. L., Hesser, J. E., Hill, G., Garlick, G. S., & O'Keefe, L. M. 1985, PASP, 97, 247
Warner, B. 1976, in IAU Symp. 73, Structure and Evolution of Close Binary Systems, ed. P. Eggleton, S. Mitton, & J. Whelan (Dordrecht: Reidel), 85
Webbink, R. F. 1976, ApJ, 209, 829
———. 1985, in IAU Symp. 113, Dynamics of Star Clusters, ed. J. Goodman & P. Hut (Dordrecht: Reidel), 541
Vandenberg, D. A., & Bell, R. A. 1985, ApJS, 58, 561
van't Veer, F. 1979, A&A, 109, 17
Verbunt, F., Hasinger, G., Johnston, H. M., & Bunk, W. 1993, in Space Astronomy, ed. J. Trumper, C. Cesarsky, G. Palumbo, & G. Bignami, Adv. Space Res., 13(12), 151
Vilhu, O. 1982, A&A, 109, 17
Yan, L., & Mateo, M. 1994, AJ, 108, 1810
Yan, L., & Reid, I. N. 1996, MNRAS, 279, 751